SUPPLEMENTARY MATERIAL ONLINE

Role of cAMP in Cardiomyocyte Viability: Beneficial or Detrimental?

Yishuai Zhang[1], Si Chen[1], Lingfeng Luo[2, 1, #], Sarah Greenly[1], Hangchuan Shi[3, 4], Jasmine Jiayuan Xu[1] and Chen Yan[1, *]

[1]Aab Cardiovascular Research Institute, Department of Medicine
[2]Department of Biochemistry and Biophysics
[3]Department of Clinical and Translational Research
[4]Department of Public Health Sciences; University of Rochester School of Medicine and Dentistry, Rochester, NY 14642.

[#] Current address is Department of Surgery, Stanford University, Stanford, CA 94305

*Correspondence to: Chen Yan, Ph.D., Aab Cardiovascular Research Institute, University of Rochester School of Medicine and Dentistry, Rochester, NY 14642. Phone: 585-276-7704. Email: Chen_Yan@urmc.rochester.edu

Short title: Role of cAMP in Cardiomyocyte Viability

Supplementary Materials and Methods

Animal studies

All experimental C57BL/6J mice were purchased from Jackson Laboratories and housed in an air-conditioned room with a 12 h light–dark cycle and fed a standard chow diet with free access to tap water. All animal experiment procedures were performed according to the guidelines of the University of Rochester Committee on Animal Resources and the NIH Guide for the Care and Use of Laboratory Animals. All mice in animal experiments were randomized using simple randomization with a specific ID number before the procedure. Experimental mice were randomly assigned to different groups and treated as indicated. The sample sizes of animal studies were estimated by G*power analysis (https://www.psychologie.hhu.de/arbeitsgruppen/allgemeine-psychologie-und-arbeitspsychologie/gpower) based on the primary parameters such as mean values and standard deviations taken from preliminary data at power 80% with an α of 0.05. For the acute cardiac injury mouse model induced by ISO, a power calculation indicated that at least 7 animals in the ISO treatment groups would be required to provide >80% power (α=0.05) to detect a 60%-70% change in IgG-positive myocardium portion with a standard deviation of ≈40% based on our pilot experiments. Because these values for the sham groups are extremely low, 3 animals would be enough. Considering the variations of PANX1(WT) or PANX1(S206A) expression levels in individual mice that affect the outcomes, the mouse numbers were almost doubled in these groups. For the acute ischemia-reperfusion (IR) mouse model, considering the possible animal mortality in experiments, a power calculation indicated that at least 8-10 animals (10 for male mice, 8 for female mice, because the possible mortality of female mice in experiments is less than that of male mice) in the IR groups would provide >80% power (α=0.05) to detect a 40%-50% change in myocardial infarction area and cardiac function with a standard deviation of ≈30% based on our pilot experiments. The variations for the sham groups are much smaller, thus at least 6 animals would be enough.

ISO-induced acute cardiac injury in mice

C57BL/6J mice aged 16-18 weeks were randomly chosen and subjected to subcutaneous injection with vehicle saline or isoproterenol (ISO, 100 mg/kg per 8 hours twice in 24 hours) as described previously with modifications [30,31]. 24 hours (h) later, mice were anesthetized via intraperitoneal injection of ketamine (80 mg/kg)/midazolam (0.6 mg/kg), and finally euthanized by cervical dislocation. Heart tissue and blood samples were collected for further analysis. The heart was stopped by injection of 10% potassium chloride (KCl) and excised. A part of heart ventricular tissue was snap-frozen in OCT for cryosectioning (5 μm), and another part was snap-frozen in liquid nitrogen and stored at -80°C for further experiments. Plasma was collected by centrifuging blood at 3500 g for 20 minutes (min) at 4°C and stored at -80°C for further experiments. We only used male mice because our pilot study showed that female mice were resistant to acute ISO-induced cardiac injury in this model (Figure S12F and S12G). There was no animal excluded from the analysis in experiments.

To determine the role of pannexin-1 (PANX1) phosphorylation at S206 in ISO-induced acute cardiac injury, we created adeno-associated virus 9 (AAV9) expression vectors expressing GFP, human wild type PANX1 (PANX1(WT)), or PANX1 mutant with Serine 206 mutated to Alanine (PANX1(S206A)) under the control of a cardiac-specific cTNT promoter. AAV9-cTNT-PANX1(WT), AAV9-cTNT-PANX1(S206A), or AAV9-cTNT-GFP virus was produced by Gene Therapy Center Vector Core of the University of North Carolina. AAV9 ($2.2X10^{11}$ vg/mouse) was intraperitoneally injected into postnatal male mice at 6-7 days as described [32,33], and mice were then kept for further studies. Mice at 16 weeks old were subjected to acute ISO treatment as

described above. There were 6 groups of mice, including Saline/GFP (n=3), ISO/GFP (n=7), Saline/PANX1(WT) (n=6), ISO/PANX1(WT) (n=14), Saline/PANX1(S206A) (n=6) and ISO/PANX1(S206A) (n=14).

Ex vivo ischemia-reperfusion (IR) in isolated mouse hearts

To evaluate the effect of e[cAMP] on IR-induced cardiac injury and the underlying mechanism, excluding the impact of other tissues or organs, we used isolated mouse hearts subjected to global ischemia and reperfusion with a Langendorff system *ex vivo* [48]. The sample sizes were determined according to our previous study [48]. There were two experiments. For experiment #1, there were two groups of mice, including IR without cAMP (n=6) and IR with cAMP (n=6). C57BL/6J male mouse at the age of 12-14 weeks was anesthetized via intraperitoneal injection of heparin and ketamine/midazolam, and the heart was isolated in a cold K-H buffer and quickly connected to Langendorff perfusion system. Under a constant perfusion pressure (80 mmHg), the heart was equilibrated with K-H buffer (95% oxygen, 5% carbon dioxide, 37°C) and then perfused with K-H buffer containing with or without cAMP (20 μM) for 30 min and through the entire reperfusion period. Then, the heart was subjected to 40 min no-flow global ischemia followed by 50 min reperfusion. At the end of reperfusion, the coronary outflow was collected for CK activity measurement. For experiment #2, there were two groups of mice, including IR with PSB36 (A1R antagonist) (n=7) and IR with PSB36 plus cAMP (n=7). C57BL/6J male mouse at the age of 12-14 weeks was anesthetized via intraperitoneal injection of heparin and ketamine/midazolam, and the heart was isolated in a cold K-H buffer and quickly connected to Langendorff perfusion system. Under a constant perfusion pressure (80 mmHg), the heart was equilibrated with K-H buffer (95% oxygen, 5% carbon dioxide, 37°C) and then perfused with K-H buffer containing PSB36 (20 nM) with or without cAMP (20 μM) for 30 min and through the entire reperfusion period. Then, the heart was subjected to 40 min no-flow global ischemia followed by 50 min reperfusion. At the end of reperfusion, the coronary outflow was collected for CK activity measurement. The heart was subjected to recycling perfusion with 2 mg/mL FITC-Dextran (40 kDa) in K-H buffer for 20 min. After Dextran perfusion, the mouse heart was stopped by 10% KCl, fixed by 4% (wt/vol) paraformaldehyde (PFA), dehydrated by 30% sucrose in PBS, freezing embedded in OCT, and cryosectioned (5 μm). The Dextran-positive myocardium area was quantified as described above. The representative images were chosen based on their quality and to most accurately reflect the group average across all the available data.

In vivo mouse cardiac ischemia-reperfusion (IR) injury

To evaluate the effect of extracellular cAMP (e[cAMP]) on IR-induced cardiac injury in mice, we used *in vivo* mouse cardiac IR model. C57BL/6J male or female mice aged 10-12 weeks were randomly chosen for cardiac IR injury or sham operation as described [48]. There were 4 groups, including sham/saline (n=6 for male or female mice), IR/saline (n=10 for male mice or n=8 for female mice), sham/cAMP (n=6 for male or female mice), and IR/cAMP (n=10 for male mice or n=9 for female mice). Briefly, mice were anesthetized with 2.0% isoflurane by endotracheal intubation performed with a 20-gauge intravenous catheter. Ischemia was performed by ligating the left anterior descending artery (LAD) at 1.5 to 2.0 mm below the left auricle. Occlusion of LAD was confirmed by the change of color and the elevation of the ST segment on the electrocardiogram. After 45 minutes (min) of occlusion, the suture was untied for reperfusion, and the chest cavity and skin incision were closed. Sham operation was performed via an identical procedure, except that the suture was just passed underneath LAD without occlusion. At the beginning of reperfusion, mice were subjected to subcutaneous injection with cAMP (10 mg/kg) or vehicle (saline). After 24 hours (h) of reperfusion, mouse cardiac function was detected by echocardiogram, and then mice were anesthetized via intraperitoneal injection of ketamine (80 mg/kg)/midazolam (0.6 mg/kg). The blood samples were collected for further experiments. LAD was re-occluded at the same position for IR surgery. The heart was perfused with 2% Evans Blue

to delineate the risk area, stopped by injection 10% KCl and sliced into 4-5 slices (1 mm), and heart tissue slices were stained with 1% 2, 3, 5-Triphenyltetrazolium chloride (TTC) for the infarct areas. The area at risk (unstained by Evans blue dye) and the myocardial infarct area (unstained by TTC) were measured using ImageJ. The infarct area/risk area ratio was used to evaluate myocardial infarction, and the risk area/total area ratio was used to evaluate the repeatability and stability of surgery. The representative images were chosen based on their quality and to most accurately reflect the group average across all the available data. The heart tissues from another pack of mice were stopped by injection of 10% KCl and snap frozen in OCT for cryosectioning (5 μm) for further experiments, including histological immunostaining and TUNEL staining. The mice were finally euthanized by cervical dislocation. The surgeries and echo assessments were processed by a surgery core technician who is blind from the grouping information and data collection. Analyses were carried out by another person. We excluded the mice that died during the ischemia surgery due to the surgery's failure.

Echocardiography

Cardiac function was evaluated via echocardiography. Mice were anesthetized via continuous inhaling isoflurane (2%) mixed with oxygen. Echocardiography was monitored in anesthetized mice using a Vevo3100 echocardiography machine equipped with an MS-550D 40-MHz frequency probe (VisualSonics). B-mode echocardiography on the long axis was used to assess ventricular function. The ejection fraction was calculated by the following formula: %EF= (LV end-diastolic volume - LV end-systolic volume)/ (LV end-diastolic volume) × 100%. The echocardiography data were collected blindly.

Plasma cardiac troponin I measurement

Plasma cardiac troponin-I (cTnI) was detected using the mouse cardiac troponin-I Elisa kit (Life Diagnostics inc, CTNI1HSP) to evaluate cardiac injury. The plasma samples were diluted by 4 folds, and the measurement was carried out as described [9]. The absorbance at 450 nm was measured in a plate reader (BMG LABTECH Inc, NC, USA). The results were calculated from the standard curve.

Creatine kinase activity measurement

Creatine kinase (CK) activity in collected coronary outflow was measured using the Creatine Kinase Activity Colorimetric Assay Kit (BioVision, K777-100) to evaluate cardiac injury in ex vivo studies [49]. At the end of heart perfusion, coronary outflow solution was collected for creatine kinase activity assay. The measurement was performed according to the manufacturer's instructions. 50 μL samples were mixed with 50 μL reaction mixture and incubated at 37°C for 40 min. OD450nm values at 10 min and 40 min were recorded by a multi-plate reader. OD450nm value at the endpoint of the standard was recorded for standard curve preparation. The results were calculated from the standard curve, reaction time, and sample volume (CK activity = NADH amount/reaction time/sample volume).

Myocardial IgG accumulation and quantification in the heart

We measured myocardial accumulation of IgG by immunostaining to evaluate myocardial cell membrane integrity associated with cardiac injury [34]. After animal sacrifice, the excised heart was frozen, embedded in OCT, and cryosectioned into 5 μm sections kept at -80°C for future experiments. Heart sections (without fixation) were dried at RT for 20 min, washed with PBS once for 2 min, and incubated with Dylight 594 conjugated goat anti-mouse IgG secondary antibody and Alexa Fluor™ 488 conjugated Wheat Germ Agglutinin (WGA) (20 μg/mL) at 4°C overnight. The sections were washed with PSB thrice for 5 min each and mounted with a gold anti-fade mounting solution. The whole heart cross-section was scanned by EVOS FL auto image system, or multiple images were taken with Olympus upright Epi-Fluorescence Microscope BX51 and

composited together. One heart section from each mouse was used. IgG-positive myocardium area with red fluorescence was analyzed by ImageJ. The result was presented as the percentage of IgG-positive myocardium versus whole heart cross-section area. The representative images were chosen based on their quality and to most accurately reflect the group average across all the available data.

TUNEL staining and quantification in the heart

Myocardial apoptosis in the heart was measured using Terminal deoxynucleotidyl transferase dUTP nick end labeling (TUNEL) staining. The frozen heart sections were dried and fixed in 4% PFA at RT for 1 h. After being washed with PBS, heart sections were permeabilized with 1% triton x-100 at RT for 1 h. The heart sections were washed with PBS and incubated with TUNEL staining buffer at 37°C for 1 h, according to the commercial kit manual (Sigma-Aldrich, 12156792910). Myocytes and nuclei were visualized respectively using a membrane staining Alexa Fluor™ 488 conjugated WGA at 20 μg/ml RT for 1 h and 4',6-diamidino-2-phenylindole (DAPI) at 1μg/mL RT for 5 min. Heart sections were mounted with a gold anti-fade mounting solution. TUNEL-positive nuclei with red fluorescence indicated apoptotic CMs. One heart section from each mouse was used. 10 fields from each heart section were randomly imaged by Olympus upright Epi-Fluorescence Microscope BX51. Approximately 1×10^4 cells from each heart section were counted using ImageJ. The result was presented as the percentage of TUNEL staining positive myocardial cells versus total myocardial cells in each heart section. The representative images were chosen based on their quality and to most accurately reflect the group average across all the available data.

Proximity ligation assay and quantification in the heart and CMs

We used proximity ligation assay (PLA) to detect PKA-mediated PANX1 phosphorylation (p-PANX1) in the heart. Mice were subjected to acute ISO treatment or cardiac IR, as indicated in the text. PLA was performed according to the commercial kit (Sigma-Aldrich, DUO92008-100RXN) protocol with some modifications. Frozen heart sections were fixed in precooled acetone at -20°C for 10 min, dried at RT for 20 min, washed with PBS 2 times for 5 min each, and permeabilized with 1% triton x-100 at RT for 1 h. Heart sections were washed with PBS 3 times for 5 min each time, blocked in Duolink blocking solution at RT for 1 h, and incubated in two primary antibodies together, e.g., mouse anti-pannexin1 antibody plus rabbit anti-Phospho-PKA Substrate (RRXS*/T*) antibody, rabbit anti-β-1AR antibody, rabbit anti-H2R antibody or rabbit anti-P2X7R antibody at 4°C overnight. Heart sections incubated with individual primary antibodies alone were used as negative controls. After washing away primary antibodies, heart sections were sequentially incubated in Duolink probe anti-rabbit plus (Sigma-Aldrich, DUO92004-100RXN) and anti-mouse minus mixture (Sigma-Aldrich, DUO92004-100RXN) at 37°C for 1 h, in ligation reaction mixture at 37°C for 30 min, and in amplification reaction mixture at 37°C for 100 min. Myocardial cells were visualized using WGA staining as described above, and then heart sections were mounted with Duolink® In Situ Mounting Medium with DAPI (Sigma-Aldrich, DUO92004-100RXN). One section from each mouse was used. 7-10 fields from each section were randomly recorded by Olympus upright Epi-Fluorescence Microscope BX51. The red fluorescence intensity of the PLA positive signal and myocardium area were analyzed by ImageJ. The result was presented as the fluorescence intensity of PLA normalized by the myocardium area. The representative images for PLA quantification experiments were chosen based on their quality and to most accurately reflect the group average across all the available data.

We also used PLA to detect PKA-mediated p-PANX1 and protein-protein interaction in isolated CMs. PLA was carried out following commercial kit instructions with some minor modifications. Isolated CMs were seeded in Laminin-coated 35-mm glass bottom dishes. For detecting PKA-mediated p-PANX1, CMs were pretreated with PKA inhibitor followed by βAR or

H2R agonist stimulation as indicated in the text. For detecting CAMKIIδ binding with calmodulin to reflect CAMKII activation [71], CMs were pretreated with PANX1 inhibitor or P2X7R antagonist followed by βAR or H2R agonist stimulation as indicated in the text. For detecting protein-protein interaction, CMs at the basal condition were used. CMs were fixed in 4% PFA at RT for 1 h, washed with PBS 3 times for 5 min each, and permeabilized with 1% triton x-100 at RT for 1 h. CMs were sequentially washed with PBS 3 times for 5 min each, blocked in Duolink blocking buffer at RT for 1 h, and incubated with two primary antibodies together as indicated in the results, including mouse anti-PANX1 antibody, rabbit anti-Phospho-PKA Substrate (RRXS*/T*) antibody, rabbit anti-CAMKIIδ antibody, mouse anti-calmodulin antibody, rabbit anti-β-1AR antibody, rabbit anti-H2R receptor antibody, rabbit anti-P2X7R antibody, rabbit anti-A2A receptor antibody, mouse anti-MRP4 antibody, rabbit anti-CGRPR antibody and rabbit anti-RXFP1 antibody at 4°C overnight. Meanwhile, CMs were incubated with each corresponding primary antibody alone as negative controls. After washing away primary antibodies, myocytes were then sequentially incubated in Duolink probe anti-rabbit plus and anti-mouse minus mixture at 37°C for 1 h, in ligation reaction mixture at 37°C for 30 min, and in amplification reaction mixture at 37°C for 100 min. Myocytes were visualized using WGA (20 μg/ml at RT for 1 h) staining and then mounted with Duolink® In Situ Mounting Medium with DAPI. For quantification, 10 fields from each dish were randomly recorded by confocal microscope in a z-stack model. The red dot indicated a PLA positive signal. Approximately 40-50 CMs per dish were counted by ImageJ. The result was presented as an average dot number per CM. The representative images for PLA quantification experiments were chosen based on their quality and to most accurately reflect the group average across all the available data.

Adult mouse CM isolation and culture

Adult mouse CM isolation and culture were performed according to our previous protocol with some modifications [9,10]. The sample sizes for *in vitro* studies were determined according to our previous experiences [9,10]. Briefly, C57BL/6J mice at 14-17 weeks were randomly chosen and anesthetized by intraperitoneal injection of heparin and ketamine (80 mg/kg)/midazolam (0.6 mg/kg). The heart was rapidly harvested and placed in precooled isolation buffer (120 mM NaCl, 15 mM KCl, 0.6 mM Na_2HPO_4, 0.6 mM KH_2PO_4, 1.2 mM $MgSO_4$, 10 mM HEPES, 10 mM creatine monohydrate, 30 mM Taurine, 5.6 mM D-glucose, 4.6 mM $NaHCO_3$, 10 mM BDM, filtered at 0.20 μm, pH 7.4) on ice to wash away blood and excess fat briefly. The heart was immediately cannulated using a blunted 20-gauge needle and connected to a Langendorff apparatus which used gravity to drive buffer heated to 37°C into the heart. The heart was initially perfused for 3 min using isolation buffer, followed by calcium-free digestion buffer (isolation buffer with 1.3 mg/mL collagenase II) for 3 min, then digestion buffer with 28 nM $CaCl_2$ for 6-10 min. Digestion was halted by removing the heart from the cannulating needle and placing it in 1 mL calcium-containing digestion buffer with 9 ml stopping buffer (isolation buffer with 10% FBS and 12.5 nM $CaCl_2$). The atria were removed, and ventricles were dissociated using forceps in a petri dish. An additional 10 ml digestion buffer was then added to the dissociated heart and filtered through 200-μm mesh into a 50 mL conical tube. The tube was then incubated for 5 min at 37°C followed by 5 min at RT, allowing a pellet to form. In sterile conditions, the supernatant, primarily cardiac fibroblasts, was retained if desired or discarded. The pellet with CMs was then resuspended in a 10 ml stopping buffer. Calcium concentration in this buffer was then gradually increased, with 2 min between each step: first to 112.5 nM, then to 512.5 nM, and finally to 1.4 μM. CMs were then visually inspected; more than 60% of myocytes retained rod-shaped morphology, then used for experiments. Myocytes were then kept at RT for 10 min to form a pellet and resuspended in CM culture medium (MEM with 0.02% BSA, 10 mM HEPES, 4 mM $NaHCO_3$, 10 mM creatine, 0.5% insulin-selenium-transferrin, 2% penicillin/streptomycin (P/S), 10 μM blebbistatin, pH 7.4). CMs were then plated on Laminin (10-20 μg/mL) coated dishes, centrifuged at 500 g for 2 min, and incubated in a cell culture incubator for 2 h. CMs were washed twice with PBS to remove dead

cells and incubated in a fresh culture medium for 1 h before treatments. CMs were cultured in the presence of blebbistatin (a myosin II inhibitor) to block myocyte contraction and to extend their survival during the culture, as described previously [9,10,62].

Trypan blue viability assay and quantification

To evaluate CM death, we performed trypan blue staining as described previously with some modifications [9]. Isolated CMs were seeded in Laminin coated 35-mm glass bottom dishes and then treated with different cell death stimuli (ISO, AMT, or H_2O_2) for 24 h with pretreatment of a vehicle or various reagents (inhibitors, antagonists, or calcium chelate) as indicated. After treatment, CMs were centrifuged at 500 g for 2 min and incubated with Trypan blue solution (final concentration of 0.2%) for 5 min. After removing the trypan blue solution, the whole glass bottom in the dish was automatically scanned with 20 fields and composited by the EVOS FL auto image system. The dead CM was stained blue. An average of 1 x 10^3 myocytes in each dish were counted using ImageJ. Some key experimental results were measured by two people, with one person counting blindly. The result was the percentage of trypan blue positive CMs versus total CMs. The representative images were chosen based on their quality and to most accurately reflect the group average across all the available data.

LDH leakage measurement

LDH leakage to the culture medium of damaged CMs was measured using the LDH Cytotoxicity Detection Kit (Takara Bio, MK401) as described [10]. After inducing CM death as indicated, the cell culture medium was centrifuged at 1 x 10^3 g for 5 min at 4°C to collect supernatant for LDH leakage measurement. Samples were incubated with a reaction mixture at RT for 30 min. OD490nm values were measured by a multi-plate reader. The results were calculated by comparing the sample OD490nm values to the control with a maximal OD490nm value derived from CMs treated with 1% Triton X-100 for 24 h to induce a maximal LDH leakage. The results were presented as the fold change of the control group.

cAMP level measurement

Intracellular or extracellular cAMP was measured using the cAMP Elisa kit (Cell Biolabs, STA-500). Each sample was collected from approximately 1.5-2 x 10^5 CMs cultured in 1 mL culture medium. CMs were pretreated with various inhibitors/antagonists followed by agonists of different GsPCRs as indicated. For intracellular cAMP measurement, CMs were lysed with lysis buffer after the treatment and centrifuged to collect the supernatant of cell lysis. To measure extracellular cAMP, the CM culture medium was collected by centrifugation and heated at 80°C for 5 min to inactivate enzymes involved in cAMP degradation. According to the cAMP assay Elisa kit manual, an acetylated sample or standard was incubated with an anti-cAMP antibody and HRP conjugated cAMP tracer at RT for 2 h in each well or the 96-well plate pre-coated with secondary antibody. Each well was washed 5 times and reacted with substrate solution at RT for 20 min. The reaction was stopped by the stopping solution. OD450nm value was recorded by a multi-plate reader. Results were calculated based on the standard curve and normalized to the protein concentration of the sample following the cAMP Elisa kit instruction using the nonacetylated protocol. For plasma cAMP measurement, each plasma sample was diluted for 2 folds by lysis buffer. Results were calculated based on the standard curve.

Extracellular ATP measurement

ATP was measured using the ATP determination kit (Thermo Fisher Scientific, A22066) based on the manual. Each sample is collected from approximately 1.5-2 x 10^5 CMs cultured in 1 mL culture medium. Since ATP was known to be rapidly degraded by ATPases such as CD39 on the extracellular membrane surface, CMs were pretreated with a CD39 inhibitor, POM1 (20 μM). At the end of treatment, the CM culture medium was immediately collected by centrifugation and

heated at 80°C for 5 min to prevent ATP degradation. Standard or experimental samples were incubated with luciferase and its substrate D-Luciferin at 28°C for 15 min. The luminescence assay was carried out by a multi-plate reader. The results were calculated by standard curve and normalized by each sample protein concentration.

Intracellular calcium measurement

We used Fluo-4 to evaluate intracellular calcium changes in CMs as described with modifications [72]. Isolated CMs were seeded in Laminin-coated 35-mm glass bottom dishes. CMs were incubated with fresh CM culturing medium containing Fluo-4 AM (10 μM) and 0.2% Pluronic F127 for 30 min to allow Fluo-4 AM loading. Then the CM culturing medium was replaced by Tyrode buffer (140 mM NaCl, 5 mM KCl, 5 mM HEPES, 1 mM NaH_2PO_4, 1 mM $MgCl_2$, 1.8 mM $CaCl_2$, 10 mM glucose, and 10 μM blebbistatin, pH=7.4) and incubated in the dark for 20 min to allow for complete de-esterification of AM esters. CMs were kept at rest for 2 min and then subjected to treatment. The fluorescence signals of Fluo-4 in CMs were continuously recorded under the excitation and emission wavelength 488/515 nm every 1 min for 40 min by the time-lapse image system. 40 CMs on average from each dish were recorded. The fluorescence intensity of Fluo-4 was analyzed using SlideBook 6.0. The relative calcium change ($\Delta F/F_0$) was calculated by the ratio of the maximal changes of Fluo-4 fluorescence intensity (ΔF) versus that at 0 min (F_0).

Pannexin-1 activity assay

We evaluated PANX1 activity in CMs by measuring YO-PRO3 influx as described with modifications [29]. Isolated CMs were seeded in Laminin coated 35-mm glass bottom dishes and transfected with lentiviral PANX1(WT) or PANX1(S206A) for 48 hr. Then the CM culturing medium was replaced by assay buffer (144 mM NaCl, 5 mM KCl, 1 mM $CaCl_2$, 1 mM $MgCl_2$, 20 mM HEPES, 2mM L-D glucose, 10 μM blebbistatin, pH=7.4) and incubated with or without ISO (10 μM) or AMT (10 μM) in the presence of YO-PRO3 (1 μM) for 20 min. The fluorescence images of YO-PRO3 in CMs were recorded under the excitation and emission wavelength 612/631 nm at 0 min and 20 min. 10 random fields with 200 CMs on average from each dish were recorded by the EVOS FL auto image system. The fluorescence intensity of YO-PRO3 was analyzed using ImageJ. The relative change of YO-PRO3 ($\Delta F/F_0$) was calculated by the ratio of maximal changes of the intensity (ΔF) versus that at 0 min (F_0). The representative images were chosen based on their quality and to most accurately reflect the group average across all the available data.

Immunoprecipitation

After the treatment, the heart tissue or CM membrane protein was extracted according to the membrane protein extraction kit (Thermo Scientific, 89842). Protease inhibitor and phosphatase inhibitor cocktails were added to the extraction buffer. We immunoprecipitated PANX1 using PANX1 antibody and immunoblotting for phosphorylated PANX1 using phosphor-PKA Substrate (RRXS*/T*) antibody. 150 μg protein was mixed with 2 μg mouse-anti pannexin1 primary antibody and 1 mg dynabeads protein G, and incubated with rotation at 4°C overnight. The beads were washed with membrane protein extraction lysis buffer 5 times and boiled with 1X loading buffer at 100°C for 7 min. The supernatant was subjected to Western blotting. The PKA phosphorylated PANX1 and total PANX1 were detected by immunoblotting with phosphor-PKA Substrate (RRXS*/T*) antibody and PANX1 antibody, respectively.

Co-immunoprecipitation

For identifying the complex of PANX1, β1AR, H2R, and P2X7R, we immunoprecipitated PANX1 from the membrane protein lysate of P2X7R overexpressed CMs using PANX1 antibody and immunoblotting PANX1, β1AR, H2R, and P2X7R using PANX1, β1AR, H2R, and P2X7R antibodies. 200 μg protein was pre-cleaned with 0.1 μg 0.5% BSA blocked TrueBlot® Anti-Rabbit

IgG Magnetic Beads for 1 hour at 4°C. Pre-cleaned protein was mixed with 4 μg rabbit anti-pannexin1 primary antibody or rabbit IgG and incubated with rotation at 4°C overnight. The protein mixture with PANX1 antibody or rabbit IgG was mixed with 0.2 μg BSA blocked TrueBlot® Anti-Rabbit IgG Magnetic Beads and incubated with rotation for 4 hours at 4°C. The beads were washed with membrane protein extraction lysis buffer 5 times and boiled with 1X loading buffer at 100°C for 7 min. The supernatant was subjected to Western blotting. The immunoblots of PANX1, β1AR, and H2R were performed using rabbit anti-PANX1 antibody, rabbit anti-β1AR antibody, rabbit anti-H2R, and Rabbit TrueBlot® Anti-Rabbit IgG HRP secondary antibody. The immunoblots of P2X7R were performed using goat anti-P2X7R antibody and Goat TrueBlot® Anti-Goat IgG HRP secondary antibody. The blot blocking and secondary antibody dilution (1:5000 diluted in blocking buffer) were performed using blocking buffer containing 5% non-fat milk in PBST (Tween 20 diluted in PBS of 0.1%). The experiment was repeated 3 times.

For identifying the complex of MRP4, A2AR, CGRP-R, and RXFP1, we immunoprecipitated MRP4 from CM membrane protein lysate using MRP4 antibody and immunoblotting MRP4, A2AR, CGRPR, and RXFP1 using MRP4, A2AR, CGRPR, and RXFP1 antibodies. 200 μg protein was pre-cleaned with 0.1 μg 0.5% BSA blocked TrueBlot® Anti-Rabbit IgG Magnetic Beads for 1 hour at 4°C. Pre-cleaned protein was mixed with 4 μg rabbit anti-MRP4 primary antibody or rabbit IgG and incubated with rotation at 4°C overnight. The protein mixture with PANX1 antibody or rabbit IgG was mixed with 0.2 μg BSA blocked TrueBlot® Anti-Rabbit IgG Magnetic Beads and incubated with rotation for 4 hours at 4°C. The beads were washed with membrane protein extraction lysis buffer 5 times and boiled with 1X loading buffer at 100°C for 7 min. The supernatant was subjected to Western blotting. The immunoblots of MRP4 and A2AR were performed using rat anti-MRP4 antibody, goat anti-rat IgG HRP secondary antibody, mouse anti-A2AR antibody, and Mouse TrueBlot® ULTRA Anti-Mouse Ig HRP secondary antibody, respectively. The immunoblots of CGRPR and RXFP1 were performed using rabbit anti-CGRPR antibody, rabbit anti-RXFP1 antibody, and Rabbit TrueBlot® Anti-Rabbit IgG HRP secondary antibody. The blot blocking and secondary antibody dilution were performed using the blocking buffer as above. The experiment was repeated 3 times.

Western blot

After the treatment, CMs were harvested and lysed in a buffer (RIPA buffer consisting of 50 mM Tris-Cl, pH 7.4, 150 mM NaCl, 1% (v/v) NP-40, 0.1% (w/v) SDS, 1 mM EDTA, pH 8.0, or solubilization buffer from membrane protein extraction kit) with protease inhibitor cocktail (working concentration: 1.04 mM AEBSF, 0.8 μM Aprotinin, 40 μM Bestatin, 14 μM E-64, 20 μM Leupeptin and 15 μM Pepstatin A) and 100X phosphatase inhibitor cocktail (contents: sodium fluoride, sodium orthovanadate, sodium pyrophosphate and β-glycerophosphate, Thermofisher Scientific) on ice for 20 min. The cell lysate was centrifuged at 16000 × g 4°C for 15 min. The supernatant was collected, mixed with loading buffer, and heated at 100°C for 7 min. The sample was loaded in 10% SDS-PAGE gel and subjected to electrophoresis in a constant voltage (110 V) model for 2 h. For detecting PANX1 protein levels in CMs overexpressing GFP, PANX1(WT), PANX1(S206A), or PANX1(S206D), or for detecting P2X7R protein levels in CMs overexpressing LacZ or hP2X7R, 15~20 μg protein per sample was loaded into the gel. After electrophoresis, the protein was transferred onto the PVDF membrane in a constant current (140 mA) model for 1 h. The blot was blocked by blocking buffer containing 5% bovine serum albumin in PBST for 1 h and incubated with the primary antibody, including rabbit anti-Phospho-PKA substrate, rabbit anti-PANX1, rabbit anti-P2X7R or mouse anti-GAPDH antibodies at 4°C overnight. The primary antibody was removed, and the blot was washed by PBST and incubated with HRP-conjugated secondary antibody (1:5000 diluted in blocking buffer) at RT for 1 h. The secondary antibody was washed away by PBST. The blot was exposed using ECL reagent (Immobilon Western Chemiluminescent HRP Substrate, Millipore, WBKLS0100) and imaged by Biorad gel dock. The

phosphorylated PANX1 level was normalized to the total PANX1, and the PANX1 or P2X7R level was normalized to GAPDH. The representative images were chosen based on their quality and to most accurately reflect the group average across all the available data.

Lentivirus production and transduction

The lentiviral expression vectors carrying human wild-type PANX1 (pLV[Exp]-Puro-CMV>hPANX1(WT)), PANX1(S206A) with serine 206 (TCT) mutated to alanine (GCC) (pLV[Exp]-Puro-CMV>hPANX1(S206A)) and PANX1(S206D) with serine 206 (TCT) mutated to aspartic acid (GAC) (pLV[Exp]-Puro-CMV>hPANX1(S206D)) were generated by Vector-Builder, and pLV[Exp]-Puro-CMV>GFP was used as negative control. The lentiviral expression vectors for shRNAs were designed with the online software from Vector-Builder and produced by Vector-Builder Inc. In lentivirus-mediated transduction, CMs were treated with lentivirus for 8 h, and the virus was washed away by fresh medium. CMs were cultured for an additional 48 h and then subjected to further treatment. The sequences of shRNA vectors are shown below.

pLV[shRNA]-EGFP-U6>mAdcy5	AGAATCACTGTTTACGGATTA
pLV[shRNA]-EGFP-U6>mAdcy6	CACCCTGATACTCGGGATTTA
pLV[shRNA]-EGFP-U6>mAbcc4 (MRP4)	GGTATACTTCAGACGGAATTA
pLV[shRNA]-EGFP-U6>mAbcc5 (MRP5)	GTGCATTC TCATCTCCAAATT
pLV[shRNA]-EGFP-U6>mEnpp1	CCAGAGACATACTATTCATTT
pLV[shRNA]-EGFP-U6>mEnpp2	CGACCCAAGATTCCCAATAAT
pLV[shRNA]-EGFP-U6>mEnpp3	CGGCAATGTATCAAGGTTTAA
pLV[shRNA]-EGFP-U6>mNt5e (CD73)	GCACTGGGAAATCATGAATTT
pLV[shRNA]-EGFP-U6>mAdora1	CATGGAGTACAT GGTCTACTT
pLV[shRNA]-EGFP-U6>mEntpd1 (CD39)	CCAAGGACATTCAGGTTTCAA
pLV[shRNA]-EGFP-U6>mPANX1	CCACCTTCGATGTTCTACATT
pLV[shRNA]-EGFP-U6>mP2RX7	CCTGGACAATCTGAGGAAATT
pLV[shRNA]-EGFP-U6>Scramble	CCTAAGGTTAAGTCGCCCTCG

Adenovirus production and transduction

Adenovirus expressing hP2X7R (Ad-P2X7R) was generated using the ViraPower Adenovirus Expression System (Invitrogen) according to the manufacturer's protocol. Adenovirus expressing LacZ (Ad-Laz) was used as a negative control. We performed Ad-P2X7R and Ad-LacZ titration. WT adult mouse CMs were respectively transduced with Ad-P2X7R (50 MOI) or Ad-Laz (50 MOI), and the virus was washed away 6 h later. CMs were further cultured for an additional 48 h and then subjected to the indicated treatment. P2X7R expressions were detected by western blot.

Reverse transcription quantification PCR

CM RNA was extracted by TRIZOL according to the manufactural protocol. 1 μg total RNA was used as the template for reverse transcription into cDNA with iScript™ Reverse Transcription Supermix (Bio-rad, 1708841). The gene expression was evaluated via real-time PCR following the kit manual (Bio-rad, 1708882). The real-time PCR was performed through Polymerase activation and DNA denaturation (95°C for 3 min), 40 times thermal cycles (Denaturation at 95°C for 10 seconds, annealing and extension at 55°C for 30 seconds). Each experiment was repeated 4 times. GAPDH was used as the housekeeping gene. Data were normalized by GAPDH. The results were presented as the fold change of the control group average. The information of PCR primes are shown below.

Gene name	Sequences	Product length (bp)
Mouse Adcy5, forward 5'-3':	ACCGCCAATGCCATAGACTT	125

Mouse Adcy5, reverse 5'-3':	TGCAGATACAGAGCCAGCAC	
Mouse Adcy6, forward 5'-3':	CGGCTCATGGAGCAGATGAA	80
Mouse Adcy6, reverse 5'-3':	GGACCCATGTTCAACCCGAT	
Mouse mAbcc4 (MRP4), forward 5'-3':	GTCAGAGGCCATCGTCAGCA	136
Mouse mAbcc4 (MRP4), reverse 5'-3':	CTTGTCCCAGAAAGCGGTGAAA	
Mouse mAbcc5 (MRP5), forward 5'-3':	CGAAGGGTTGTGTGGATCTTTTG	142
Mouse mAbcc5 (MRP5), reverse 5'-3':	GGTTAGACTCTGTTGCCTGGGTG	
Mouse ENPP1, forward 5'-3':	AGACGACTGCAAAACCCACA	128
Mouse ENPP1, reverse 5'-3':	GTGATTCAAACTCTGCTGGACAC	
Mouse ENPP2, forward 5'-3':	TGATAAGGTAGAGCCAAAGAACA	99
Mouse ENPP2, reverse 5'-3':	GCAGGTCGTCCATACAGGAG	
Mouse ENPP3, forward 5'-3':	GCACTACAGAATACGCCTGG	71
Mouse ENPP3, reverse 5'-3':	GCAACCTCGCCTTCGCTA	
Mouse Nt5e (CD73), forward 5'-3':	TCCTGCAAGTGGGTGGAATC	105
Mouse Nt5e (CD73), reverse 5'-3':	AGATGGGCACTCGACACTTG	
Mouse Adora1, forward 5'-3':	GTGATTTGGGCTGTGAAGGT	142
Mouse Adora1, reverse 5'-3':	AGTAGGTCTGTGGCCCAATG	
Mouse PANX1, forward 5'-3':	ACTGTGGCTGCACAAGTTCT	85
Mouse PANX1, reverse 5'-3':	AGAGAAGCGCCAGAAGAGTG	
Mouse P2X7R, forward 5'-3':	GGGGTGACGAAGTTAGGACA	110
Mouse P2X7R, reverse 5'-3':	ACTTGGCCTTCTGACTTGACA	
Mouse Entpd1 (CD39), forward 5'-3':	ATCACCTTCGTGCCCCAAAA	169
Mouse Entpd1 (CD39), reverse 5'-3':	CGCCACCACTTGAAACCTGA	
Mouse GAPDH, forward 5'-3':	TCAAGAAGGTGGTGAAGCA	100
Mouse GAPDH, reverse 5'-3':	TGGGAGTTGCTGTTGAAGTC	

Statistical analysis

The specific sample size for each group is provided in the corresponding figure legends. Data are presented as mean ± SEM. The normality assumptions were assessed in accordance with our prior similar studies [73,74], initially tested using the Shapiro-Wilk test, and further validated through examination of residuals via q-q plots. In cases where the sample size was insufficient to ascertain normality (e.g., group n < 6), a non-parametric test was employed. To evaluate the equality of variances, the Brown-Forsythe test was applied. Consequently, the following statistical approaches were utilized: (1) Normally distributed data with equal variance were analyzed using the unpaired t-tests for two independent groups or the one-way/two-way ANOVA followed by post-hoc comparisons for three or more groups. (2) Normally distributed data rejecting equal variance were analyzed employing the Welch's t-test for two independent groups or the Welch ANOVA with Dunnett T3 post hoc tests for three or more groups. (3) Data with undetermined normal distribution underwent analysis using the Mann-Whitney test for two independent groups or the Kruskal-Wallis test with post-hoc Conover-Iman test for three or more groups. (4) When focusing on two conditions and normal data distribution remained undetermined, a two-way Aligned Ranks Transformation (ART) ANOVA was conducted. Bonferroni corrections were applied to control type I error inflation in multiple post-hoc comparisons, with corresponding adjusted P-values reported. All multiple comparisons were conducted within the same test; no experiment-wide multiple tests were applied in this study. Both parametric and non-parametric tests were two-sided, with a significance level set at 5%. The ART ANOVA models and Conover-Iman tests were executed using the ARTool and conover.test packages, respectively, in R 4.2.3 (https://www.R-project.org/). All other statistical analyses were performed using GraphPad Prism 9.0. Additional details regarding the statistical methods can be found in the figure legends.

Reagents and kits

^{10}PANX (ApexBio, A2700)
A804598 (Cayman Chemical Company, 20060)
Amthamine dihydrobromide (Tocris, 0668)
Apyrase (Sigma-Aldrich, A6535-200UN)
ATP Determination Kit (Thermo Fisher Scientific, A22066)
Autocamtide-2-related inhibitory peptide myristoylated (Tocris, 5959)
Blebbistatin (Cayman Chemical Company, 13013)
Bovine Serum Albumin (Sigma-Aldrich, A9647)
cAMP (Cayman Chemical Company, 18820)
cAMP Colorimetric ELISA Kit (Cell Biolabs, STA-500)
Ceefourin1 (Tocris, 5867)
CGP20712 (Tocris, 1024)
collagenase type II (Worthington Biochemical, LS004176)
Creatine Kinase (CK) Activity Colorimetric Assay Kit (BioVision, K777-100)
CV1808 (Tocris, 1710)
Deaminase (Sigma-Aldrich, 10102105001)
Dextran 40 (Sigma-Aldrich, FD40)
DMEM (Corning, 15017CV)
Duolink® In Situ Detection Reagents Red (Sigma-Aldrich, DUO92008-100RXN)
Duolink® In Situ Mounting Medium with DAPI (Sigma-Aldrich, DUO82040-5ML)
Duolink® In Situ PLA® Probe Anti-Mouse MINUS, Affinity purified Donkey anti-Mouse IgG (Sigma-Aldrich, DUO92004-100RXN)
Duolink® In Situ PLA® Probe Anti-Rabbit PLUS, Affinity purified Donkey anti-Rabbit IgG (Sigma-Aldrich, DUO92002-100RXN)
Duolink® In Situ Wash Buffers, Fluorescence (Sigma-Aldrich, DUO82049-4L)
ENPP1 inhibitor c (Cayman Chemical Company, 29809)
EGTA (Sigma-Aldrich, 324626-25GM)
Famotidine (Tocris, 7290)
Fetal Bovine Serum (Thermo Fisher Scientific, 10437028)
Fluo-4 AM (Ion Biosciences, 1041C)
Gap 26 (Cayman Chemical Company, 36625)
Halt™ Phosphatase Inhibitor Cocktail (100X)(Thermo Fisher Scientific, 78420)
Human CGRP8-37 (Tocris, 1181)
Human α-CGRP (Tocris, 3012)
ICI118,551 (Tocris, 0821)
In Situ Cell Death Detection Kit, TMR red (Sigma-Aldrich, 12156792910)
Insulin-Transferrin-Selenium (ITS -G) (100X) (Thermo Fisher Scientific, 41400045)
Immobilon Western Chemiluminescent HRP Substrate (Millipore, WBKLS0100)
iQ™ SYBR® Green Supermix (Bio-rad, 1708882)
iScript™ Reverse Transcription Supermix (Bio-rad, 1708841)
Isoprenaline hydrochloride (Sigma-Aldrich, I5627)
KN 92 (Tocris, 4130)
KN 93 (Tocris, 1278)
Laminin (VWR, 47743-734)
LDH Cytotoxicity Detection Kit (Takara Bio, MK401)
LY294002 (Tocris, 1130)
MEM (Thermo Fisher Scientific, 11095080)
MK-571 (Tocris, 2338)
MOUSE CARDIAC TROPONIN-I ELISA (Life diagnostics inc, CTNI1HSP)
Novex DYNAL Dynabeads Protein (Thermo Fisher Scientific, G 10-003-D)

Penicillin-Streptomycin (10,000 U/mL) (Thermo Fisher Scientific, 15140122)
Pierce™ Mem-PER™ Plus Membrane Protein Extraction Kit (Thermo Scientific, 89842)
PKI 14-22 (Tocris, 2546)
Pluronic F127 (Sigma-Aldrich, P2443)
POM1 (Tocris, 2689)
PolyJet In Vitro DNA Transfection Reagent (SignaGen Laboratories, SL100688)
Protease Inhibitor Cocktail (Sigma-Aldrich, P8340)
PSB12379 (Cayman Chemical Company, 28446)
PSB36 (Tocris, 2019)
Relaxin-2 (Sigma-Aldrich, SRP3147)
RIPA buffer (VWR, N653)
S32826 (Cayman Chemical Company, 13664)
scrambled ^{10}PANX (ApexBio, A2701)
TCS2510 (Tocris, 4069)
TrueBlot® Anti-Rabbit IgG Magnetic Beads (Rockland, 00-1800-20)
TRIZOL (Thermo Fisher Scientific, 15596026)
Trypan blue (ICN Biomedicals Inc, 194600)
Wheat Germ Agglutinin, Alexa Fluor™ 488 Conjugate (Thermo Fisher Scientific, W11261)
YO3-PRO3 (Thermo Fisher Scientific, Y3607)
Zinterol hydrochloride (Sigma-Aldrich, Z4402)
ZM241385 (Tocris, 1036)

Antibodies

Rabbit anti-A2AR antibody (Alomone Labs, AAR-002) for PLA 1:100
Mouse anti-A2AR antibody (Santa Cruz, sc-32261) for co-ip 1:200
Rabbit anti-β1AR antibody (Alomone Labs, AAR-023) for PLA 1:100
Rabbit anti-β1AR antibody (Proteintech, 28323-1-AP) for co-ip 1:1000
Mouse anti-cAMP antibody (Novus Biologicals, MAB2146)
Rabbit anti-CaMKIIδ antibody (ABclonal, A0656) for PLA 1:100
Mouse anti-Calmodulin antibody (Thermo Fisher Scientific, MA3-917) for PLA 1:100
Rabbit anti-CGRPR antibody (Novus Biologicals, NLS6731) for PLA 1:50
Rabbit anti-CGRPR antibody (ABclonal, A11979) for co-ip 1:1000
Mouse anti-GAPDH antibody (MilliporeSigma, MAB374) for Western blot 1:5000
Rabbit anti-H2R antibody (ABclonal, A14170) for PLA 1:100, for co-ip 1:1000
Rabbit anti-MRP4 antibody (AssayGenie, CAB2198)
Rat anti-MRP4 antibody (Novus Biologicals, NBP1) for co-ip 1:1000
Mouse anti-MRP4 antibody (Santa Cruz, sc-376262) for PLA 1:50
Rabbit anti-P2X7R antibody (Alomone Labs, APR-008) for western blot 1:1000
Goat anti-P2X7R antibody (Abcam, ab93354) for co-ip 1:1000
Mouse anti-pannexin-1 antibody (Novus Biologicals, MAB7097) for PLA 1:100
Rabbit anti-pannexin-1 antibody (Proteintech, 12595-1-AP) for western blot 1:1000
Rabbit anti-Phospho-PKA substrate (RRXS*/T*) antibody (Cell Signaling, 96245) for PLA 1:100, for western blot 1:1000
Rabbit anti-RXFP1 antibody (Proteintech, 18419-1-AP) for PLA 1:50
Rabbit anti-RXFP1 antibody (ABclonal, A7127) for co-ip 1:1000
Goat anti-Mouse IgG (H+L) cross-adsorbed secondary antibody, DyLight 594 conjugated (Thermo fisher Scientific, 35510) for immunostaining 1:100
Goat TrueBlot®: Anti-Goat IgG HRP (Rockland, 18-8814-31) for co-ip 1:5000
Mouse TrueBlot® ULTRA: Anti-Mouse Ig HRP (Rockland, 18-8817-30) for co-ip 1:5000
Mouse IgG HRP Linked Whole Ab (Millipore Sigma, GENA931) for western blot 1:5000
Rabbit TrueBlot®: Anti-Rabbit IgG HRP (Rockland, 18-8816-31) for co-ip 1:5000

Rabbit IgG HRP Linked Whole Ab (Millipore Sigma, GENA934) for western blot 1:5000
Anti-rat IgG, HRP-linked Antibody (Cell Signaling, 7077s) for co-ip 1:5000

Figure S1

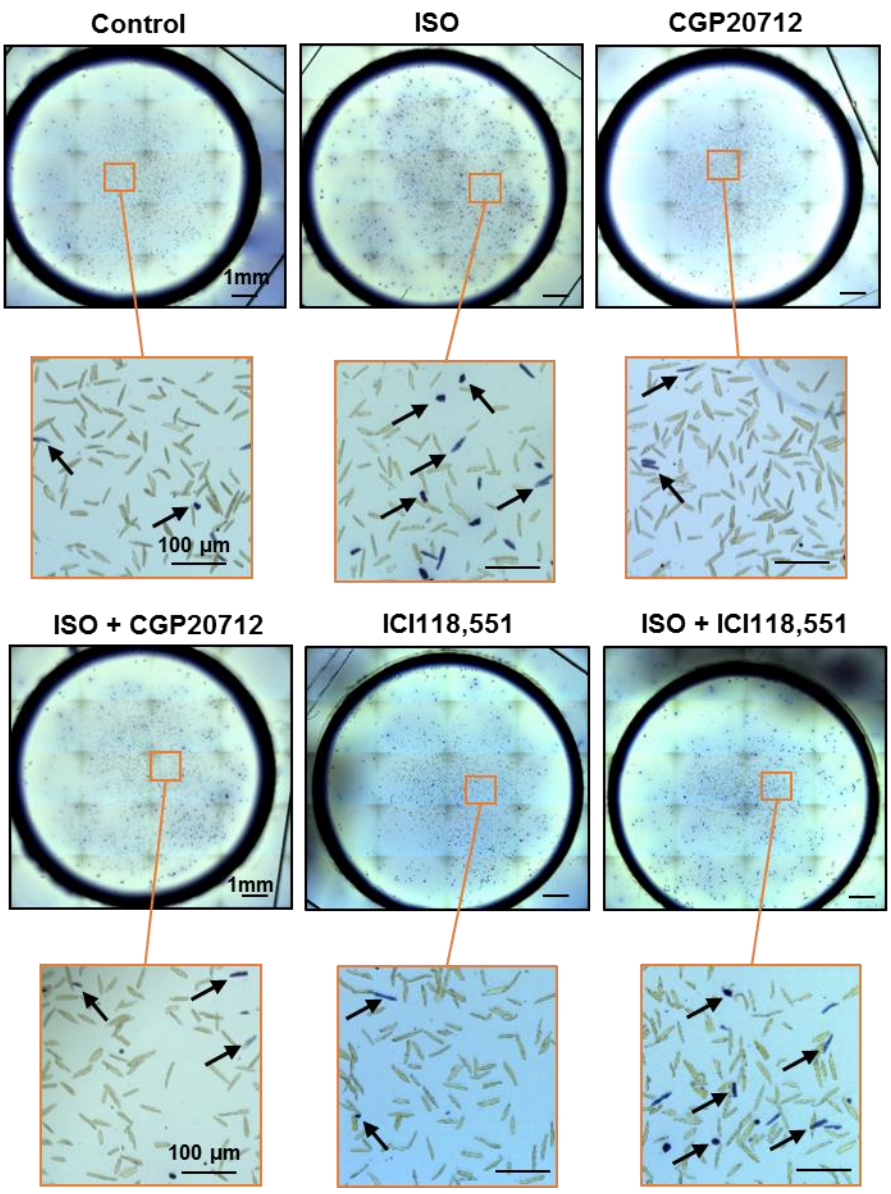

Figure S1. Images of trypan blue exclusion assay.
Low magnification images showing adult mouse CMs with trypan blue exclusion assay on an entire field of the glass-bottom dish, which were composited together from 20 fields/each dish captured by EVOS FL auto image system. Approximately 1 x 10^3 CMs were used in each dish to quantify CM death. The images with orange borders are the corresponding zoomed areas. Black arrows indicate the trypan blue stained CMs (dead CM). CMs were treated with 10 μM ISO in the presence or absence of β1AR antagonist CGP20712 (0.5 μM), β2AR antagonist ICI118,551 (0.5 μM), or vehicle for 24 h. n = independent CM isolations from 4 mice. The representative images were chosen based on their quality and to most accurately reflect the group average across all the available data.

Figure S2

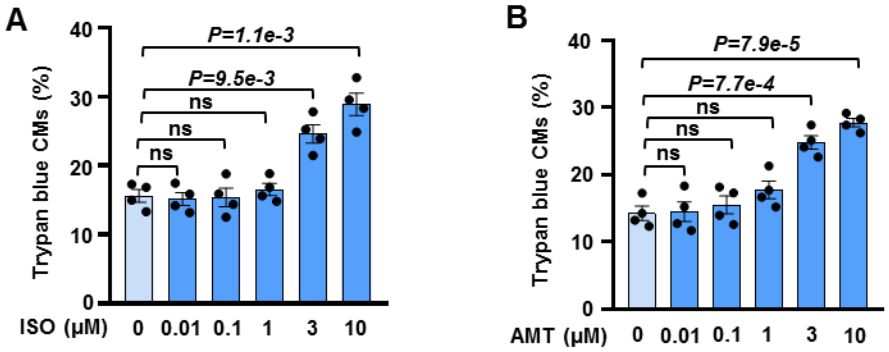

Figure S2. The dose-response studies of βAR and H2R agonists on CM death.
A, Quantitative result of trypan blue exclusion assay showing that βAR agonist ISO induced CM death in a dose-dependent manner, n=4. **B**, Quantitative result of trypan blue exclusion assay showing that H2R agonist AMT induced CM death in a dose-dependent manner, n=4. Data were presented as mean ± SEM. Data in **Figures S2A** and **S2B** were analyzed by the Kruskal-Wallis test followed by Conover-Iman post-hoc test with Bonferroni corrections for 5 comparisons. All reported P-values have been adjusted for a predetermined number of multiple comparisons, as specified in the corresponding figures. P <0.05 was statistically significant. ns: no significant difference.

Figure S3

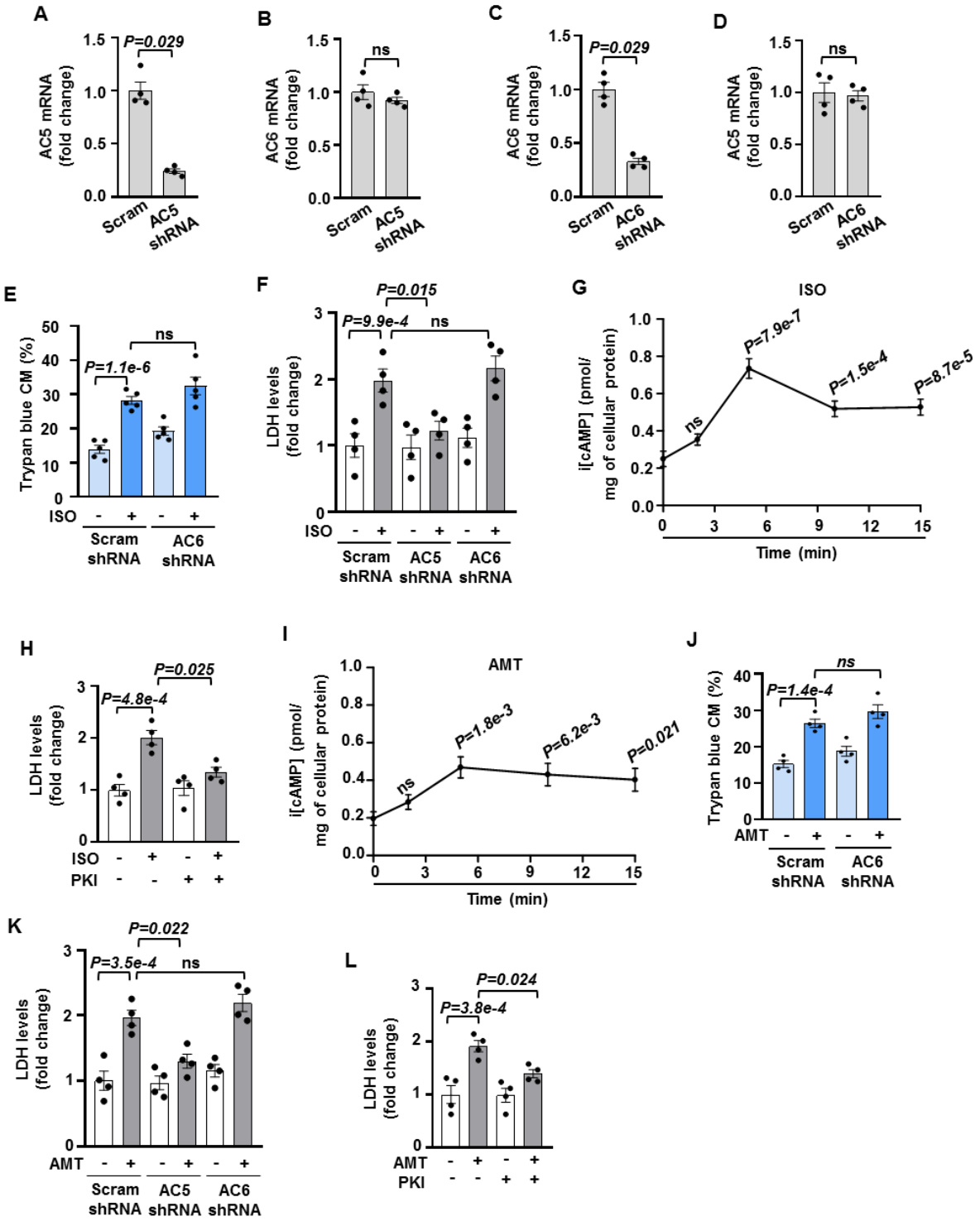
A
AC5 mRNA (fold change)
P=0.029
Scram
AC5 shRNA
B
AC6 mRNA (fold change)
ns
Scram
AC5 shRNA
C
AC6 mRNA (fold change)
P=0.029
Scram
AC6 shRNA
D
AC5 mRNA (fold change)
ns
Scram
AC6 shRNA
E
Trypan blue CM (%)
P=1.1e-6
ns
ISO
Scram shRNA
AC6 shRNA
F
LDH levels (fold change)
P=0.015
P=9.9e-4
ns
ISO
Scram shRNA
AC5 shRNA
AC6 shRNA
G
ISO
i[cAMP] (pmol/ mg of cellular protein)
ns
P=7.9e-7
P=1.5e-4
P=8.7e-5
Time (min)
H
LDH levels (fold change)
P=0.025
P=4.8e-4
ISO
PKI
I
AMT
i[cAMP] (pmol/ mg of cellular protein)
ns
P=1.8e-3
P=6.2e-3
P=0.021
Time (min)
J
Trypan blue CM (%)
ns
P=1.4e-4
AMT
Scram shRNA
AC6 shRNA
K
LDH levels (fold change)
P=0.022
P=3.5e-4
ns
AMT
Scram shRNA
AC5 shRNA
AC6 shRNA
L
LDH levels (fold change)
P=0.024
P=3.8e-4
AMT
PKI

Figure S3. The role of AC5 or AC6 in β1AR- and H2R-induced CM death; the time course of β1AR- and H2R-induced i[cAMP] changes in CMs.

A-D, Results of RT-qPCR showing mRNA levels of AC5 or AC6 in CMs treated with AC5 or AC6 shRNA lentivirus. AC5 shRNA largely reduced AC5 expression but did not affect AC6 expression, and AC6 shRNA largely reduced AC6 expression but did not affect AC5 expression. These results demonstrated the efficiency and specificity of AC5 and AC6 expression knockdown, n=4. Data were normalized by the housekeeping gene GAPDH. The results were presented as the fold change of the control group average. **E** and **J**, Quantitative trypan blue exclusion assay results show that AC6 shRNA did not significantly affect CM death induced by ISO (10 μM) or AMT (10 μM) for 24 h, n=5 for **E** and 4 for **J**. **F** and **K**, Results of LDH levels showing that AC5 shRNA, but not AC6 shRNA, attenuated ISO- or AMT-induced CM LDH leakage, n=4. **G** and **I**, Time course of i[cAMP] levels induced by ISO (10 μM) or AMT (10 μM) as indicated. ISO- or AMT-induced i[cAMP] peaked at 5 min. The statistics were performed by comparing to the 0-min time point, n=4. **H** and **L**, Result of LDH levels in CM supernatants showing that PKA inhibitor PKI 14-22 (PKI, 5 μM) significantly reduced LDH leakage induced by ISO (10 μM) or AMT (10 μM) for 24 h, n=4. Data were presented as mean ± SEM. Data in **Figures S3F** and **S3K** were analyzed by the Kruskal-Wallis test followed by Conover-Iman post-hoc test with Bonferroni corrections for 3 comparisons, **Figures S3G** and **S3I** by the Kruskal-Wallis test followed by Conover-Iman post-hoc test with Bonferroni corrections for 4 comparisons, **Figures S3E**, **S3H**, **S3J** and **S3L** by the two-way ART ANOVA with Bonferroni post-hoc test corrections for 2 comparisons, and **Figures S3A-S3D** by the Mann-Whitney test. All reported P-values have been adjusted for a predetermined number of multiple comparisons, as specified in the corresponding figures, except in **Figures S3A-S3D** where raw P-values are reported. $P < 0.05$ was statistically significant. ns: no significant difference.

Figure S4

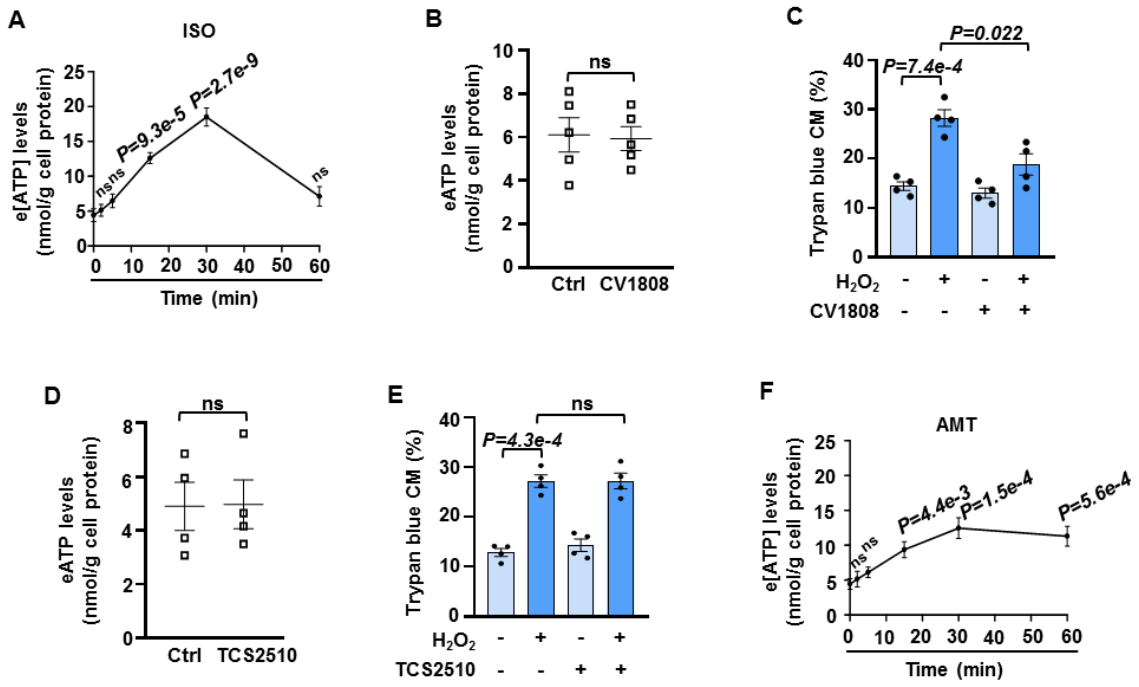

Figure S4. Time course of β1AR- and H2R-induced e[ATP] in CMs; the effect of A2R or EP4 receptor agonist on CM viability and e[ATP] levels.

A, Time course study showing e[ATP] levels induced by ISO (10 μM) as indicated. ISO-induced e[ATP] reached a peak at 30 min, n=6. The statistics were performed by comparing to the 0-min time point. **B**, Results of e[ATP] levels in CM supernatants showing that A2R agonist CV1808 (1 μM for 30 min) did not significantly affect ATP efflux from CMs, n=5. **C**, Quantitative results of trypan blue exclusion showing that CV1808 (1 μM) significantly inhibited CM death induced by H_2O_2 (5 μM for 24 h), n=4. **D**, Results of e[ATP] levels in CM supernatants showing that EP4 receptor agonist TCS2510 (1 μM) did not significantly affect ATP efflux from CMs, n=4. **E**, Quantitative results of trypan blue exclusion assay show that TCS2510 (1 μM) did not affect H_2O_2-induced CM death, n=4. **F**, Time course study showing e[ATP] levels induced by AMT (10 μM) as indicated. AMT sustainedly increased e[ATP], n=4. The statistics were performed by comparing to the 0-min time point. Data were mean ± SEM. Data in **Figure S4A** was analyzed by the one-way ANOVA followed by post-hoc comparisons with Bonferroni corrections for 5 comparisons, **Figures S4C** and **S4E** by the two-way ART ANOVA with Bonferroni post-hoc test corrections for 2 comparisons, **Figures S4B** and **S4D** by the Mann-Whitney test, and **Figure S4F** by the Kruskal-Wallis test followed by Conover-Iman post-hoc test with Bonferroni corrections for 5 comparisons. All reported P-values have been adjusted for a predetermined number of multiple comparisons, as specified in the corresponding figures, except in **Figures S4B** and **S4D** where raw P-values are reported. P <0.05 was statistically significant. ns: no significant difference.

Figure S5

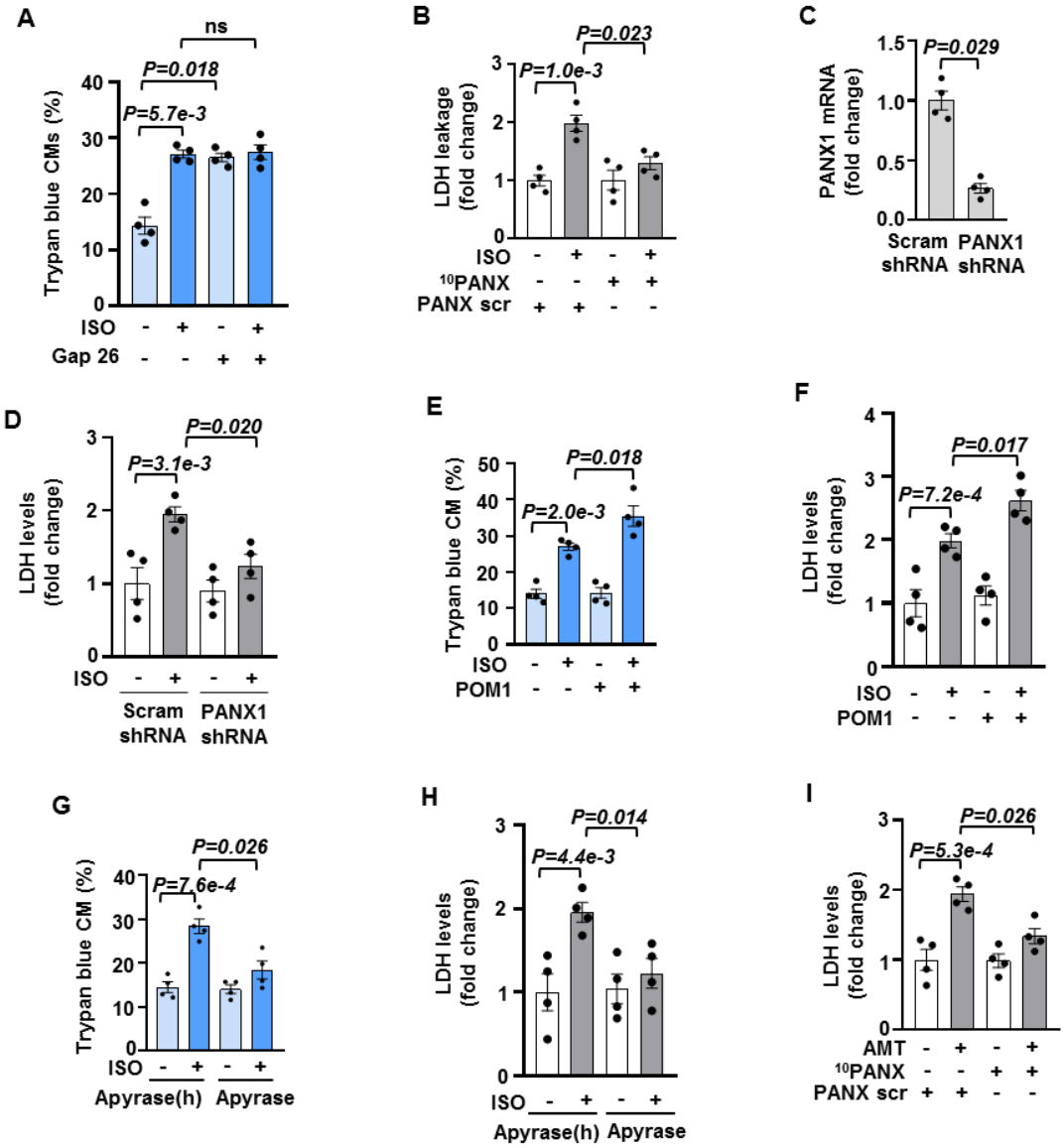
A
Trypan blue CMs (%)
ns
P=0.018
P=5.7e-3
ISO
Gap 26
B
LDH leakage (fold change)
P=0.023
P=1.0e-3
ISO
10PANX
PANX scr
C
PANX1 mRNA (fold change)
P=0.029
Scram shRNA
PANX1 shRNA
D
LDH levels (fold change)
P=0.020
P=3.1e-3
ISO
Scram shRNA
PANX1 shRNA
E
Trypan blue CM (%)
P=0.018
P=2.0e-3
ISO
POM1
F
LDH levels (fold change)
P=0.017
P=7.2e-4
ISO
POM1
G
Trypan blue CM (%)
P=0.026
P=7.6e-4
ISO
Apyrase(h)
Apyrase
H
LDH levels (fold change)
P=0.014
P=4.4e-3
ISO
Apyrase(h)
Apyrase
I
LDH levels (fold change)
P=0.026
P=5.3e-4
AMT
10PANX
PANX scr

Figure S5. The effect of connexin 43 inhibitor, PANX1 inhibitor, PANX1 shRNA, CD39 inhibitor, or ATPase on β1AR- and H2R-induced CM death.

A, Quantitative results of trypan blue exclusion showing that connexin 43 (Cx43) inhibitor Gap 26 (100 μM) directly induced CM death but did not alter CM death induced by ISO (10 μM for 24 h), n=4. **B**, Results of LDH levels in CM supernatants showing that LDH leakage induced by ISO (10 μM for 24 h) was largely reduced by PANX1 peptide inhibitor ^{10}PANX (100 μM) but not scramble peptide (PANX scr, 100 μM), n=4. **C**, Results of RT-qPCR showing mRNA levels of PANX1 in CMs treated with PANX1 shRNA lentivirus. PANX1 shRNA largely reduced PANX1 mRNA expression in CMs, n=4. Data were normalized by the housekeeping gene GAPDH. The result was presented as the fold change of the control group average. **D**, Results of LDH leakage showing that PANX1 shRNA largely reduced ISO-induced LDH leakage, n=4. **E** and **F**, Quantitative results of trypan blue exclusion and LDH leakage showing that CD39 inhibitor POM1 (20 μM) enhanced ISO-induced CM death and LDH leakage, n=4. **G** and **H**, Quantitative results of trypan blue exclusion and LDH leakage showing that depleting e[ATP] with active apyrase (2 U/mL) largely inhibited ISO-induced CM death and LDH leakage. Heat inactivate apyrase (h) was used as a negative control, n=4. **I**, Results of LDH levels in CM supernatants showing that LDH leakage induced by H2R agonist AMT (10 μM for 24 h) was largely reduced by ^{10}PANX but not PANX scr, n=4. Data were mean ± SEM. Data in **Figure S5A** was analyzed by the two-way ART ANOVA with Bonferroni post-hoc test corrections for 3 comparisons, **Figures S5B** and **S5D-S5I** by the two-way ART ANOVA with Bonferroni post-hoc test corrections for 2 comparisons, and **Figure S5C** by the Mann-Whitney test. All reported P-values have been adjusted for a predetermined number of multiple comparisons, as specified in the corresponding figures, except in **Figure S5C,** where raw P-value is reported. $P < 0.05$ was statistically significant. ns: no significant difference.

Figure S6

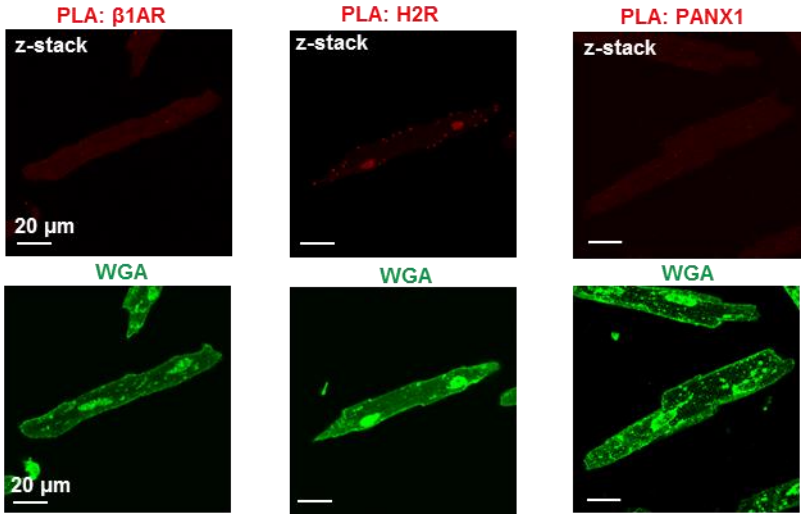

Figure S6. PLA images of negative controls for PANX1, β1AR, or H2R in CMs.
PLA results show negative controls performed with β1AR, H2R, or PANX1 antibody alone in CMs. WGA images showing CMs in the corresponding fields. There was no significant PLA signal detected in negative controls.

Figure S7

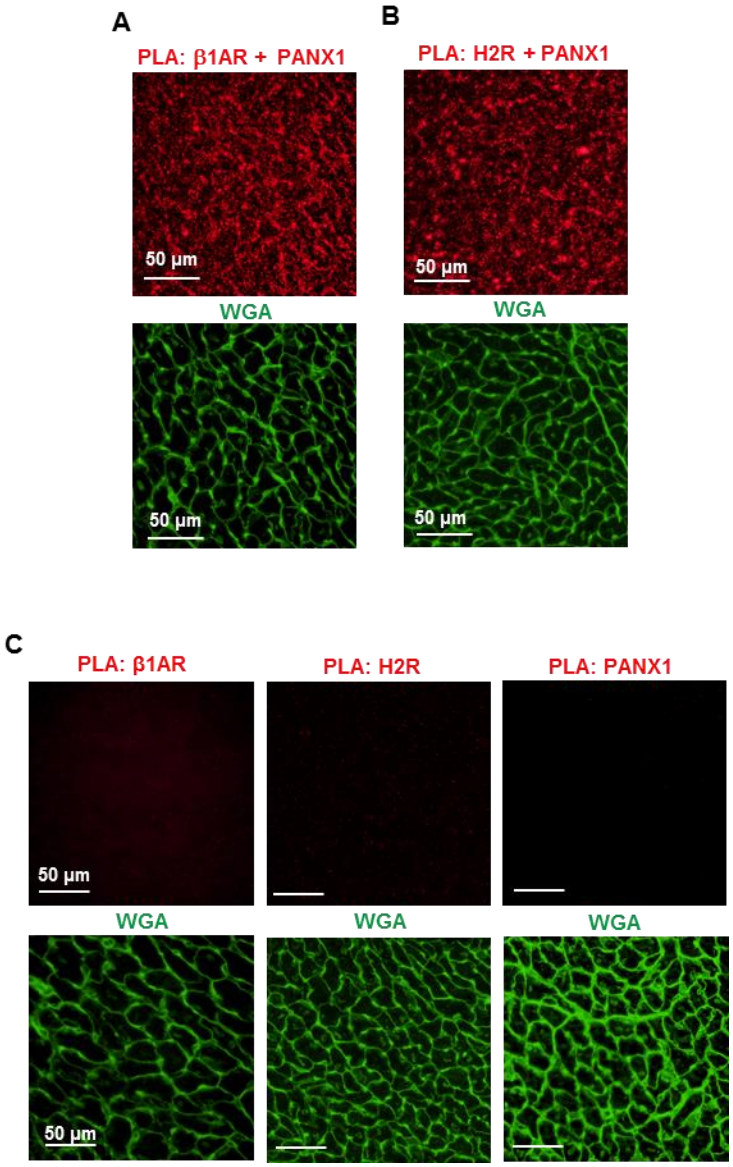

Figure S7. PLA images of PANX1 with β1AR or H2R in the heart.
A and **B**, Images of PLA performed with PANX1 plus β1AR or H2R antibodies in heart sections. There were significant red PLA positive signals detected in the heart. WGA images showing myocardium in the corresponding fields. **C**, PLA results showing negative controls performed with β1AR, H2R, or PANX1 antibody alone in heart sections. WGA images showing myocardium in the corresponding fields. There was no significant PLA signal detected in negative controls.

Figure S8

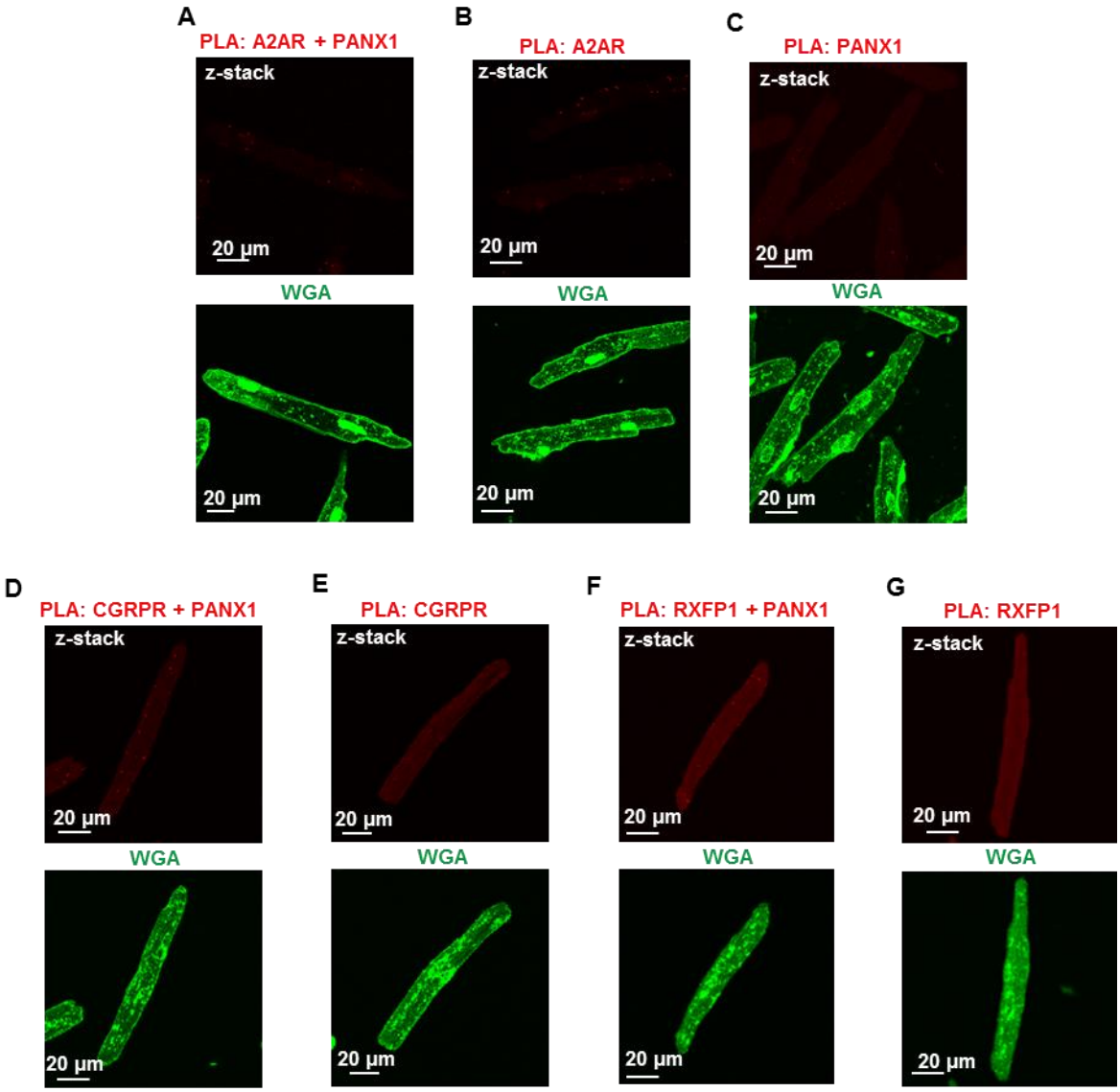

Figure S8. PLA images of PANX1 with A2AR, CGRPR, or RXFP1 and their negative controls in CMs.

A, **D,** and **F**, Images of PLA performed with PANX1 plus A2AR, CGRPR, or RXFP1 antibodies together in CMs. WGA images showing CMs in the corresponding fields. No significant PLA positive signals detected PANX1 with A2AR, CGRPR, or RXFP1, indicating no apparent interaction between PANX1 and A2AR, CGRPR, or RXFP1 detected. **B**, **C**, **E,** and **G**, PLA results showing negative controls performed with A2AR, PANX1, CGRPR, or RXFP1 antibody alone in CMs. WGA images showing CMs in the corresponding fields. There was no significant PLA signal detected in negative controls.

Figure S9

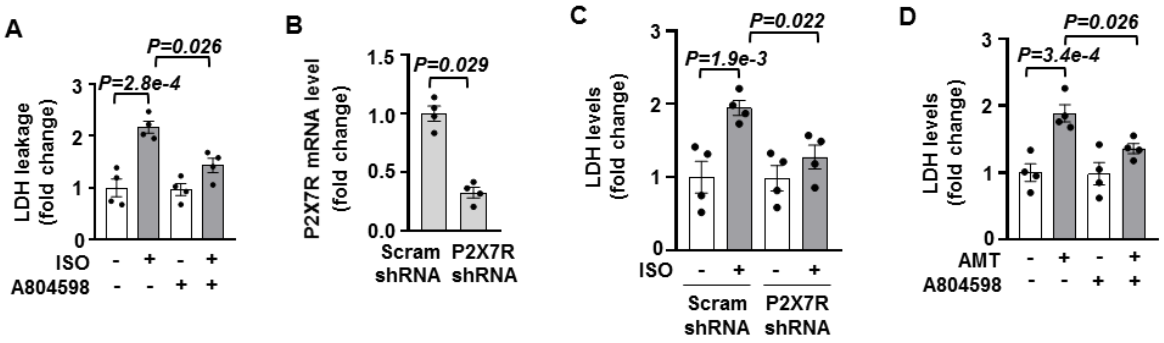

Figure S9. The role of P2X7R in β1AR- or H2R-induced CM death using P2X7R shRNA or antagonist.

A, Results of LDH levels in CM supernatants showing that P2X7R antagonist A804598 (1 μM) significantly inhibited LDH leakage induced by ISO (10 μM for 24 h), n=4. **B**, Results of RT-qPCR showing mRNA levels of P2X7R in CMs treated with P2X7R shRNA lentivirus. P2X7R shRNA largely reduced P2X7R mRNA expression in CMs, n=4. Data were normalized by the housekeeping gene GAPDH. The result was presented as the fold change of the control group average. **C**, Results of LDH leakage showing that P2X7R shRNA largely reduced ISO-induced LDH leakage, n=4. **D**, Results of LDH levels in CM supernatants showing that A804598 largely inhibited AMT-induced LDH leakage, n=4. Data were presented as mean ± SEM. Data in **Figures S9A**, **S9C,** and **S9D** were statistically analyzed by the two-way ART ANOVA with Bonferroni post-hoc test corrections for 2 comparisons, and **Figure S9B** by the Mann-Whitney test. All reported P-values have been adjusted for a predetermined number of multiple comparisons, as specified in the corresponding figures, except in **Figure S9B,** where raw P-value is reported. $P < 0.05$ was statistically significant.

Figure S10

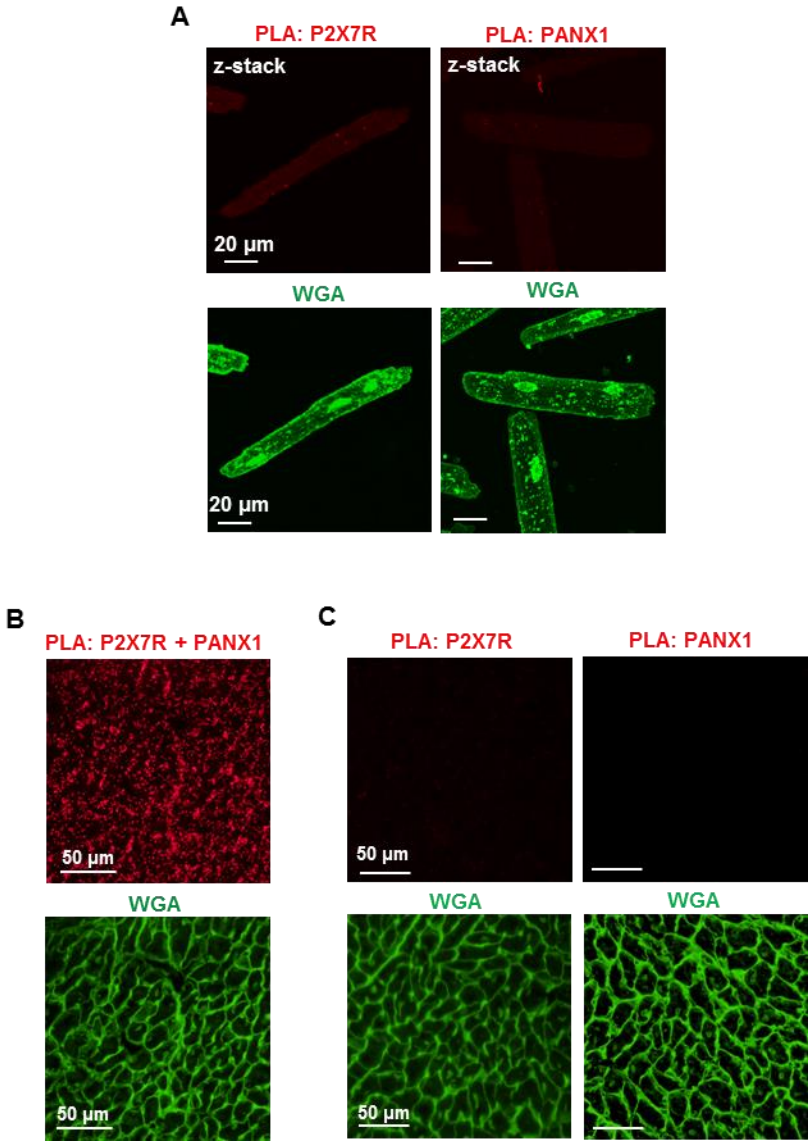

Figure S10. PLA images of PANX1 with P2X7R and their negative controls in CMs or hearts. **A**, PLA results showing negative controls performed with P2X7R or PANX1 antibody alone in CMs. WGA images showing CMs in the corresponding fields. There was no significant PLA signal detected in negative controls. **B**, Image of PLA performed by P2X7R plus PANX1 antibodies together in heart sections. There were significant red PLA positive signals detected in the heart. WGA image showing myocardium in the corresponding fields. **C**, PLA results showing negative controls performed with P2X7R or PANX1 antibody alone in heart sections. WGA image showing myocardium in the corresponding fields. There was no significant PLA signal detected in negative controls.

Figure S11

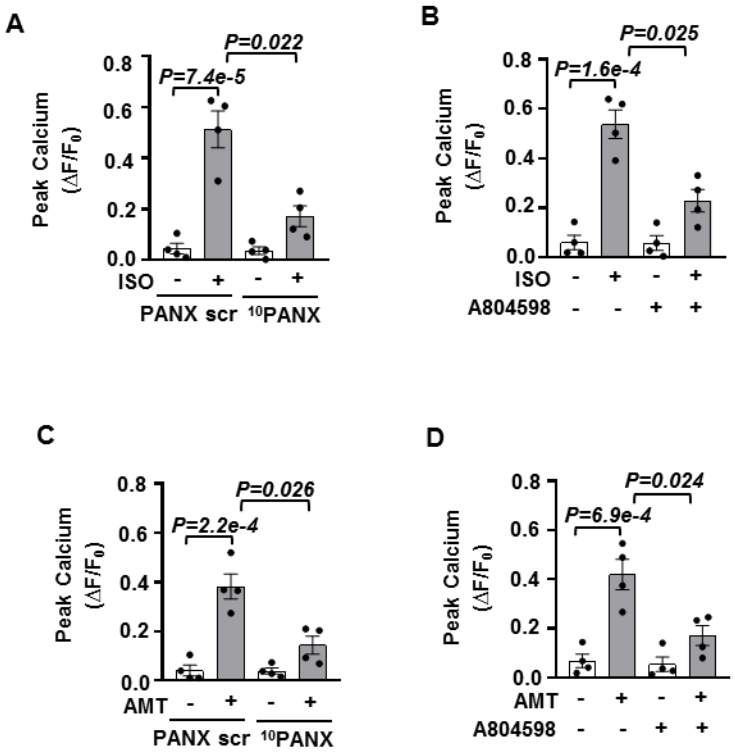

Figure S11. The role of PANX1 or P2X7R in β1AR- or H2R-induced calcium change in CMs. Fluo-4 was used for evaluating intracellular calcium change in CMs; the result was calculated as the peak change of Fluo-4 fluorescence intensity versus that at 0 min ($\Delta F/F_0$). Approximately 40 CMs from each sample were used for data collection. **A** and **C**, Results of calcium changes show that ISO (10 μM) or AMT (10 μM) significantly increased intracellular calcium in CMs, which was largely reduced by PANX1 peptide inhibitor ^{10}PANX (100 μM) but not scramble peptide (PANX scr, 100 μM), n=4. **B** and **D**, Results of calcium changes show that ISO-or AMT-induced calcium was largely reduced by P2X7R antagonist A804598 (1 μM), n=4. Data were presented as mean ± SEM. Data in **Figures S11A-S11D** were statistically analyzed by the two-way ART ANOVA with Bonferroni post-hoc test corrections for 2 comparisons. All reported P-values have been adjusted for a predetermined number of multiple comparisons, as specified in the corresponding figures. P <0.05 was statistically significant.

Figure S12

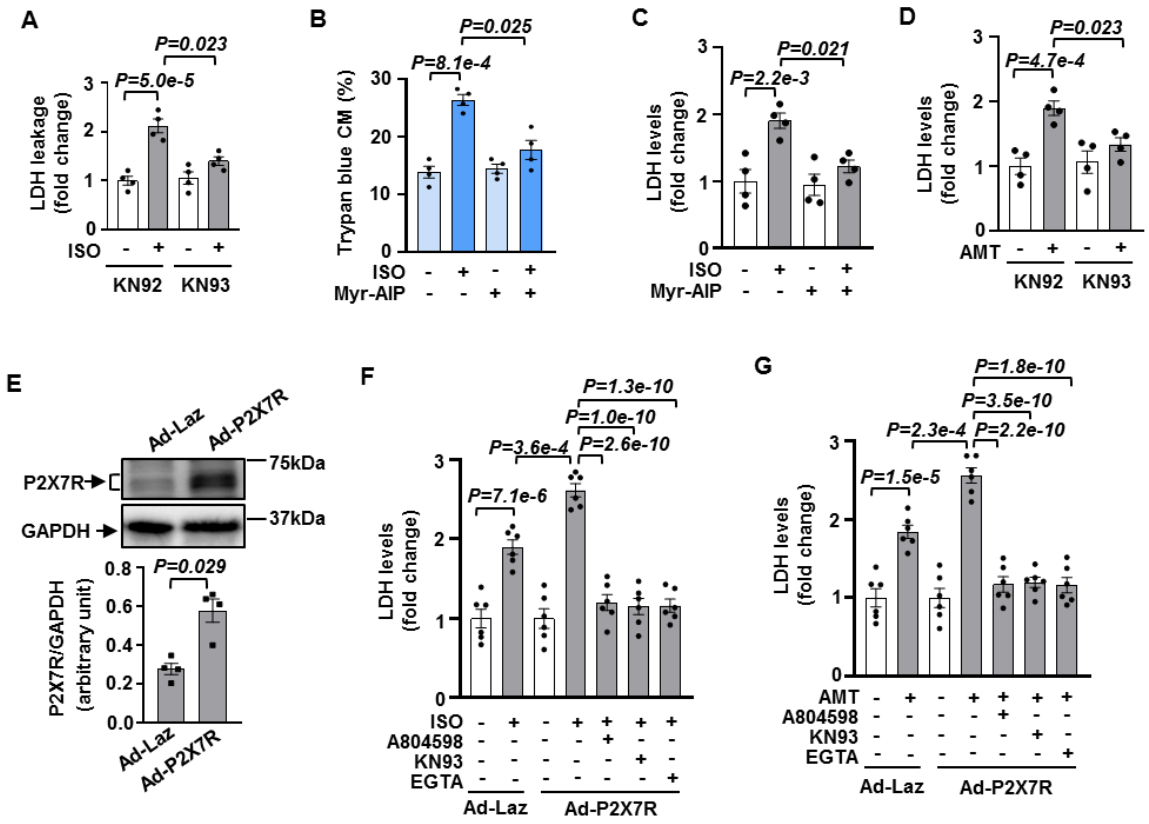
A
LDH leakage (fold change)
P=0.023
P=5.0e-5
ISO
KN92
KN93
B
Trypan blue CM (%)
P=0.025
P=8.1e-4
ISO
Myr-AIP
C
LDH levels (fold change)
P=0.021
P=2.2e-3
ISO
Myr-AIP
D
LDH levels (fold change)
P=0.023
P=4.7e-4
AMT
KN92
KN93
E
Ad-Laz
Ad-P2X7R
P2X7R
GAPDH
75kDa
37kDa
P2X7R/GAPDH (arbitrary unit)
P=0.029
F
LDH levels (fold change)
P=1.3e-10
P=1.0e-10
P=3.6e-4
P=2.6e-10
P=7.1e-6
ISO
A804598
KN93
EGTA
Ad-Laz
Ad-P2X7R
G
LDH levels (fold change)
P=1.8e-10
P=3.5e-10
P=2.3e-4
P=2.2e-10
P=1.5e-5
AMT
A804598
KN93
EGTA
Ad-Laz
Ad-P2X7R

Figure S12. The effect of CaMKII or P2X7R inhibition on β1AR- or H2R-induced CM death; the effect of P2X7R overexpression on β1AR- or H2R-induced CM death.
A and **D**, Results of LDH leakage showing that CaMKII inhibitor KN93 (2 μM) significantly reduced LDH leakage induced by ISO (10 μM for 24 h) or AMT (10 μM for 24 h) in CMs, but the control inhibitor KN92 (2 μM) did not, n=4. **B** and **C**, Results of trypan blue exclusion assay and LDH leakage showing that CaMKII peptide inhibitor myr-AIP (autocamtide-2-related inhibitory peptide myristoylated, 2 μM) inhibited ISO-induced CM death and LDH leakage, n=4. **E**, Results of P2X7R protein levels showing that P2X7R protein expression was largely increased in CMs treated with human P2X7R adenovirus (Ad-P2X7R) compared with Laz adenovirus (Ad-LacZ), n=4. Data were normalized to GAPDH. **F** and **G**, Effects of A804598 (1 μM), KN93 or calcium chelate EGTA (1 μM) on ISO- or AMT-induced LDH leakage in CMs ectopically expressing Laz or human P2X7R via adenovirus. P2X7R overexpression via adenovirus enhanced ISO- or AMT-induced LDH leakage, and P2X7R inhibition, CaMKII inhibition, or calcium chelate largely blocked ISO- or AMT-induced LDH leakage, n=6. The representative images were chosen based on their quality and to most accurately reflect the group average across all the available data. Data were presented as mean ± SEM. Data in **Figures S12F** and **S12G** were statistically analyzed by the one-way ANOVA followed by post-hoc comparisons with Bonferroni corrections for 5 comparisons, **Figures S12A-S12D** by the two-way ART ANOVA with Bonferroni post-hoc test corrections for 2 comparisons, and **Figure S12E** by the Mann-Whitney test. All reported P-values have been adjusted for a predetermined number of multiple comparisons, as specified in the corresponding figures, except in **Figure S12E,** where raw P-value is reported. $P < 0.05$ was statistically significant.

Figure S13

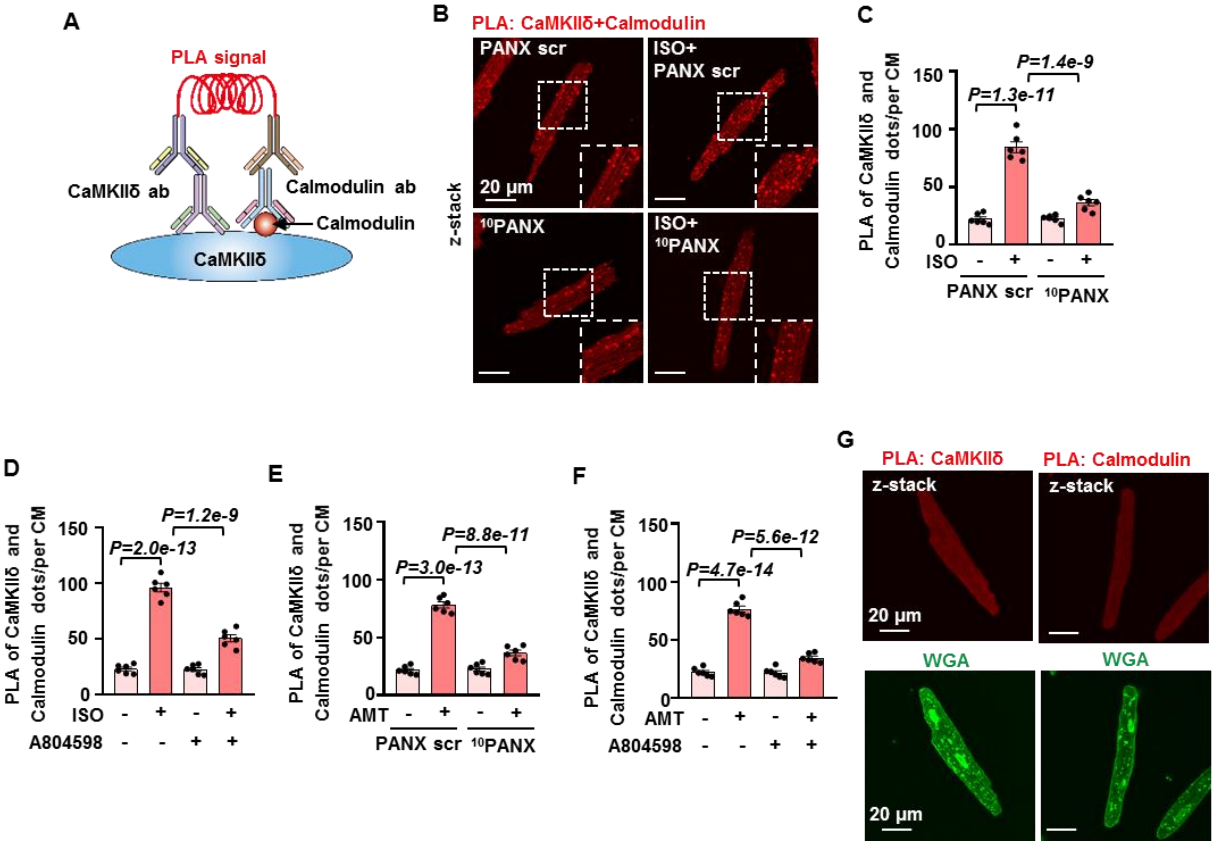
A
PLA signal
CaMKIIδ ab
Calmodulin ab
Calmodulin
CaMKIIδ
B
PLA: CaMKIIδ+Calmodulin
PANX scr
ISO+
PANX scr
z-stack
20 µm
10PANX
ISO+
10PANX
C
PLA of CaMKIIδ and
Calmodulin dots/per CM
P=1.4e-9
P=1.3e-11
150
100
50
0
ISO - + - +
PANX scr 10PANX
D
P=1.2e-9
P=2.0e-13
ISO - + - +
A804598 - - + +
E
P=8.8e-11
P=3.0e-13
AMT - + - +
PANX scr 10PANX
F
P=5.6e-12
P=4.7e-14
AMT - + - +
A804598 - - + +
G
PLA: CaMKIIδ
PLA: Calmodulin
z-stack
20 µm
WGA

Figure S13. The role of PANX1 and P2X7R in β1AR- or H2R-induced CaMKII activation. **A**, Schematic diagram showing the PLA principle for detecting CaMKIIδ binding with calmodulin to reflect CaMKII activation using CaMKIIδ and calmodulin antibodies. **B** and **C**, PLA images and quantitative results showing CaMKIIδ binding with calmodulin in CMs treated with ISO (10 μM for 30 min) with PANX1 peptide inhibitor ^{10}PANX (100 μM) or scramble peptide (PANX scr, 100 μM). Insets are zoomed areas with white dash lines. ISO significantly induced CaMKIIδ binding with calmodulin in CMs, and 10PANX, but not PANX scr, largely inhibited ISO-induced CaMKIIδ binding with calmodulin, n=6. **D**, Quantitative results showing that P2X7R antagonist A804598 (1 μM) largely inhibited ISO-induced CaMKIIδ binding with calmodulin, n=6. **E**, Quantitative results showing that AMT (10 μM for 30 min) significantly stimulated CaMKIIδ binding with calmodulin in CMs, and 10PANX, but not PANX scr, largely inhibited AMT-induced CaMKIIδ binding with calmodulin, n=6. **F**, Quantitative results showing that A804598 largely inhibited AMT-induced CaMKIIδ binding with calmodulin, n=6. **G**, Images of PLA negative controls performed by CaMKIIδ or calmodulin antibody alone in CMs. WGA images showing CMs in the corresponding fields. There was no significant PLA signal detected in negative controls. The representative images of PLA quantitative results were chosen based on their quality and to most accurately reflect the group average across all the available data. Data were presented as mean ± SEM. Data in **Figures S13C-S13F** were statistically analyzed by the two-way ANOVA followed by post-hoc comparisons with Bonferroni corrections for 2 comparisons. All reported P-values have been adjusted for a predetermined number of multiple comparisons, as specified in the corresponding figures. $P < 0.05$ was statistically significant.

Figure S14

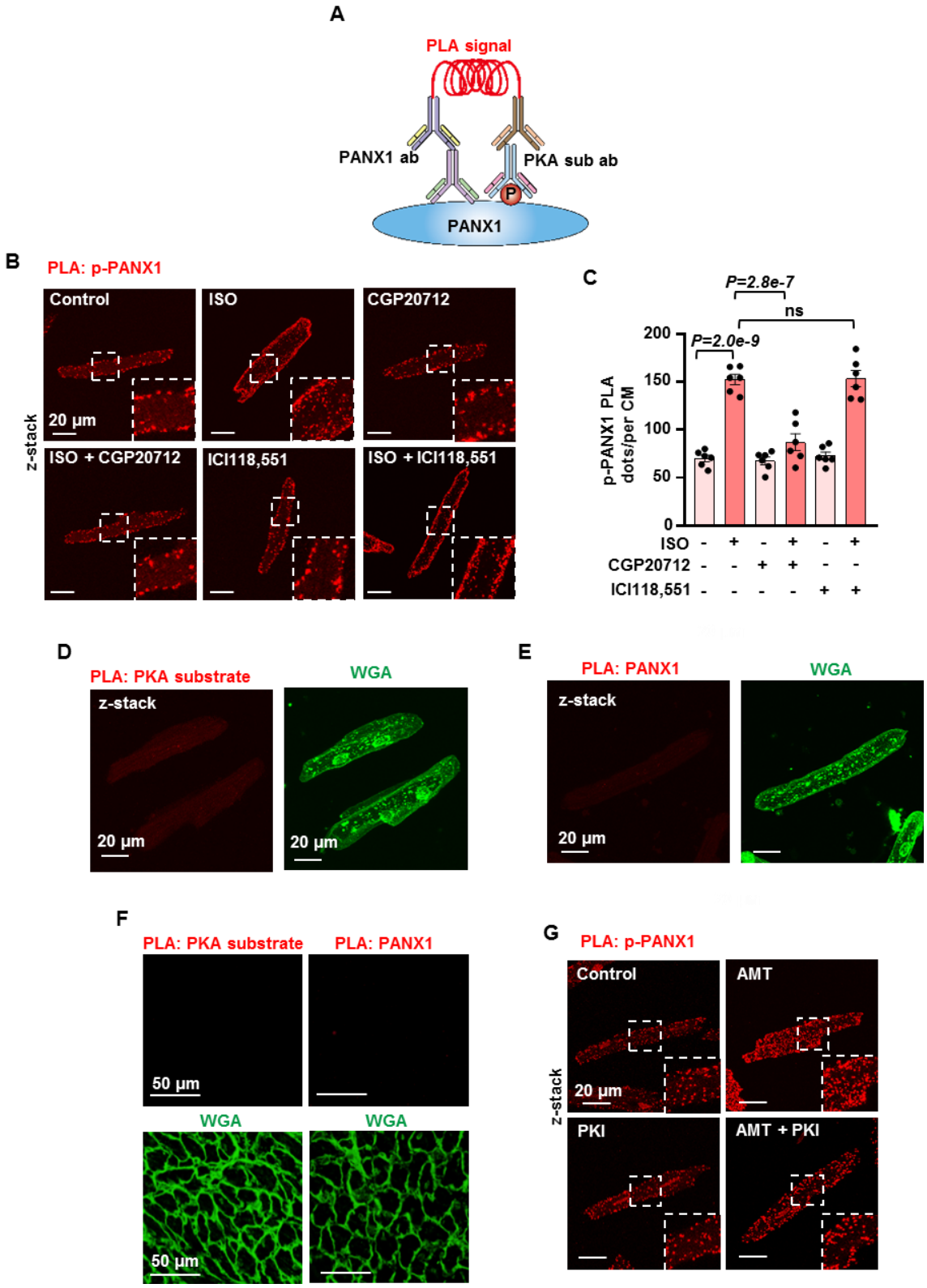
A
PLA signal
PANX1 ab
PKA sub ab
P
PANX1
B
PLA: p-PANX1
Control
ISO
CGP20712
ISO + CGP20712
ICI118,551
ISO + ICI118,551
z-stack
20 µm
C
P=2.8e-7
ns
P=2.0e-9
p-PANX1 PLA dots/per CM
200
150
100
50
0
ISO - + - + - +
CGP20712 - - + + - -
ICI118,551 - - - - + +
D
PLA: PKA substrate
WGA
z-stack
20 µm
20 µm
E
PLA: PANX1
WGA
z-stack
20 µm
F
PLA: PKA substrate
PLA: PANX1
50 µm
WGA
WGA
50 µm
G
PLA: p-PANX1
Control
AMT
z-stack
20 µm
PKI
AMT + PKI

Figure S14. The role of β1AR or β2AR in ISO-induced PKA-mediated PANX1 phosphorylation in CMs; PLA negative controls for PANX1 phosphorylation in CMs and heart; PLA results of PANX1 phosphorylation induced by AMT.

A, Schematic diagram showing the PLA principle for detecting PANX1 phosphorylation using PANX1 and PKA-substrate antibodies. **B** and **C**, PLA images and quantitative results showing PKA-mediated PANX1 phosphorylation in CMs treated with ISO (10 μM for 30 min) with or without β1AR antagonist CGP20712 (0.5 μM) or β2AR antagonist ICI118,551 (0.5 μM). Insets are zoomed areas with white dash lines. β1AR inhibition, but not β2AR inhibition, significantly reduced ISO-induced p-PANX1, n=6. **D** and **E**, Images of PLA negative controls performed by PKA substrate or PANX1 antibody alone in CMs. WGA images showing CMs in the corresponding fields. There was no significant PLA signal detected in negative controls. **F**, PLA results showing negative controls performed with PKA substrate or PANX1 antibody alone in heart sections. WGA images showing myocardium in the corresponding fields. There was no significant PLA signal detected in the heart. **G**, PLA images showing PKA-mediated PANX1 phosphorylation in CMs treated with H2R agonist AMT (10 μM for 30 min) with or without PKA inhibitor PKI (5 μM). Insets are zoomed areas with white dash lines, n=6. The representative images of PLA quantitative results were chosen based on their quality and to most accurately reflect the group average across all the available data. Data were presented as mean ± SEM. Data in **Figure S14C** was statistically analyzed by the one-way ANOVA followed by post-hoc comparisons with Bonferroni corrections for 3 comparisons. All reported P-values have been adjusted for a predetermined number of multiple comparisons, as specified in the corresponding figures. $P < 0.05$ was statistically significant. ns: no significant difference.

1544

Figure S15

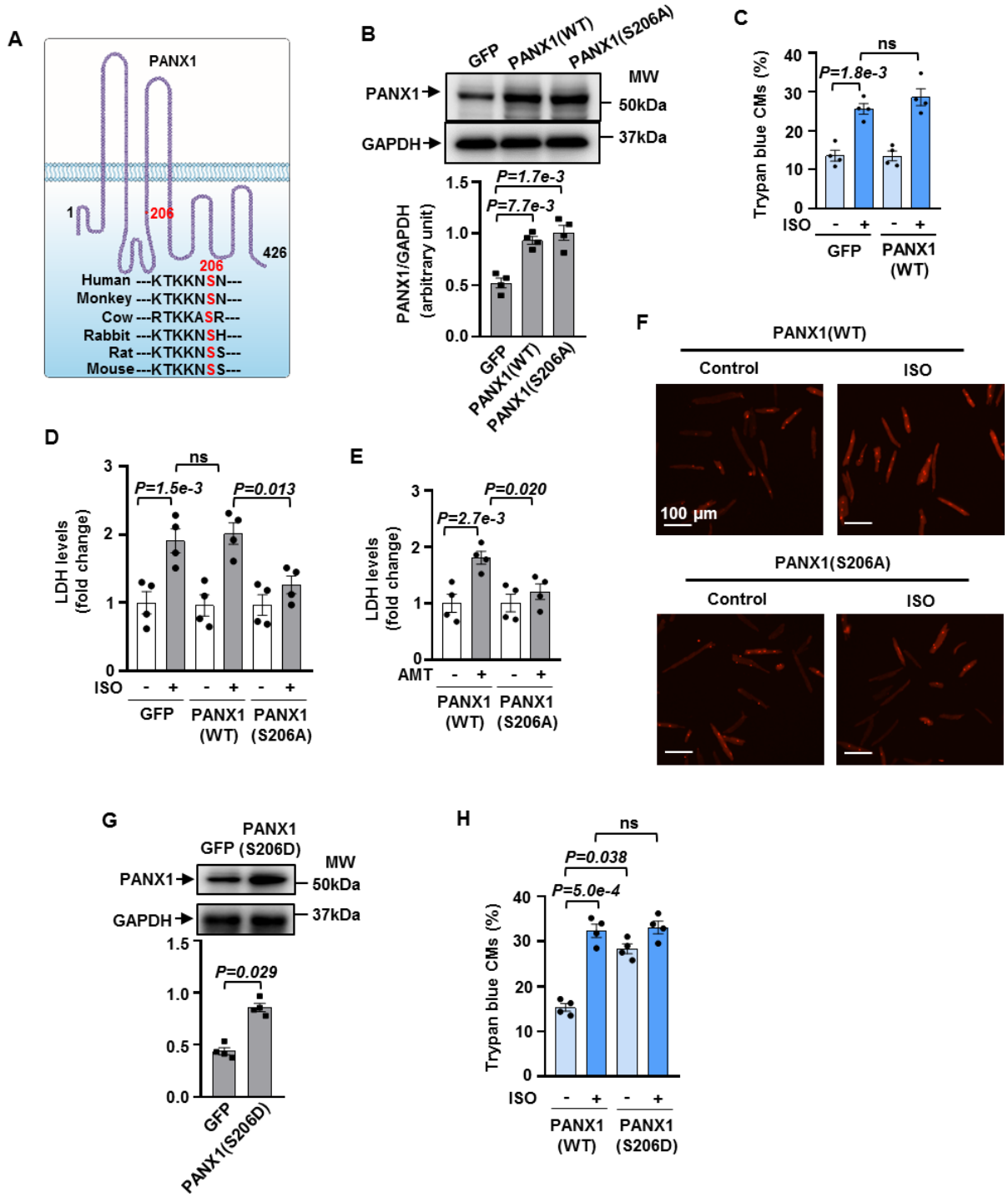

Figure S15. The role of PANX1 phosphorylation at Ser206 in βAR- or H2R-induced CM death and PANX1 activation.

A, Diagram showing the PANX1 structure with a putative PKA phosphorylation site at Ser206 that is conserved among different species. **B**, Western blots and quantitative results showing PANX1 protein levels in CMs treated with GFP, PANX1(WT), or PANX1(S206A) lentivirus. PANX1(WT) and PANX1(S206A) lentivirus increased PANX1 protein to similar levels in CM total lysates, n=4. Data were normalized to GAPDH. **C**, Quantitative results of trypan blue exclusion assay showing that CM death induced by ISO (10 μM for 24 h) was similar in CMs expressing GFP or PANX1(WT) via lentivirus, n=4. **D**, Results of LDH leakage showing that ISO-induced LDH leakage was similar in CMs expressing GFP or PANX1(WT) via lentivirus, and LDH leakage was significantly reduced in CMs expressing PANX1(S206A) via lentivirus, n=4. **E**, Results of LDH leakage showing that LDH leakage induced by H2R agonist AMT (10 μM for 24 h) was significantly attenuated in CMs expressing PANX1(S206A) via lentivirus, n=4. **F**, Representative images of YO-PRO3 (1 μM) influx in CMs transfected with PANX1(WT) or PANX1(S206A) lentivirus in the presence or absence of ISO (10 μM) for 20 min. The cellular red signals in CMs reflected YO-PRO3 influx. An average of 200 CMs/each isolation was counted to evaluate YO-PRO3 influx, n=6. **G**, Western blots and quantitative results showing PANX1 protein levels in CMs treated with GFP or PANX1(S206D) lentivirus. PANX1(S206D) lentivirus increased PANX1 protein in CM total lysates, n=4. Data were normalized to GAPDH. **H**, Quantitative results of trypan blue exclusion showing that PANX1(S206D) expression directly induced CM death but did not alter ISO-induced CM death, n=4. The representative images were chosen based on their quality and to most accurately reflect the group average across all the available data. Data were presented as mean ± SEM. Data in **Figure S15B** was analyzed by the Kruskal-Wallis test followed by Conover-Iman post-hoc test with Bonferroni corrections for 2 comparisons, **Figure S15D** by the Kruskal-Wallis test followed by Conover-Iman post-hoc test with Bonferroni corrections for 3 comparisons, **Figures S15C**, **S15E** by the two-way ART ANOVA with Bonferroni post-hoc test corrections for 2 comparisons, **Figure S15H** by the two-way ART ANOVA with Bonferroni post-hoc test corrections for 3 comparisons, and **Figure S15G** by the Mann-Whitney test. All reported P-values have been adjusted for a predetermined number of multiple comparisons, as specified in the corresponding figures, except in **Figure S15G** where raw P-value is reported. $P < 0.05$ was statistically significant. ns: no significant difference.

Figure S16

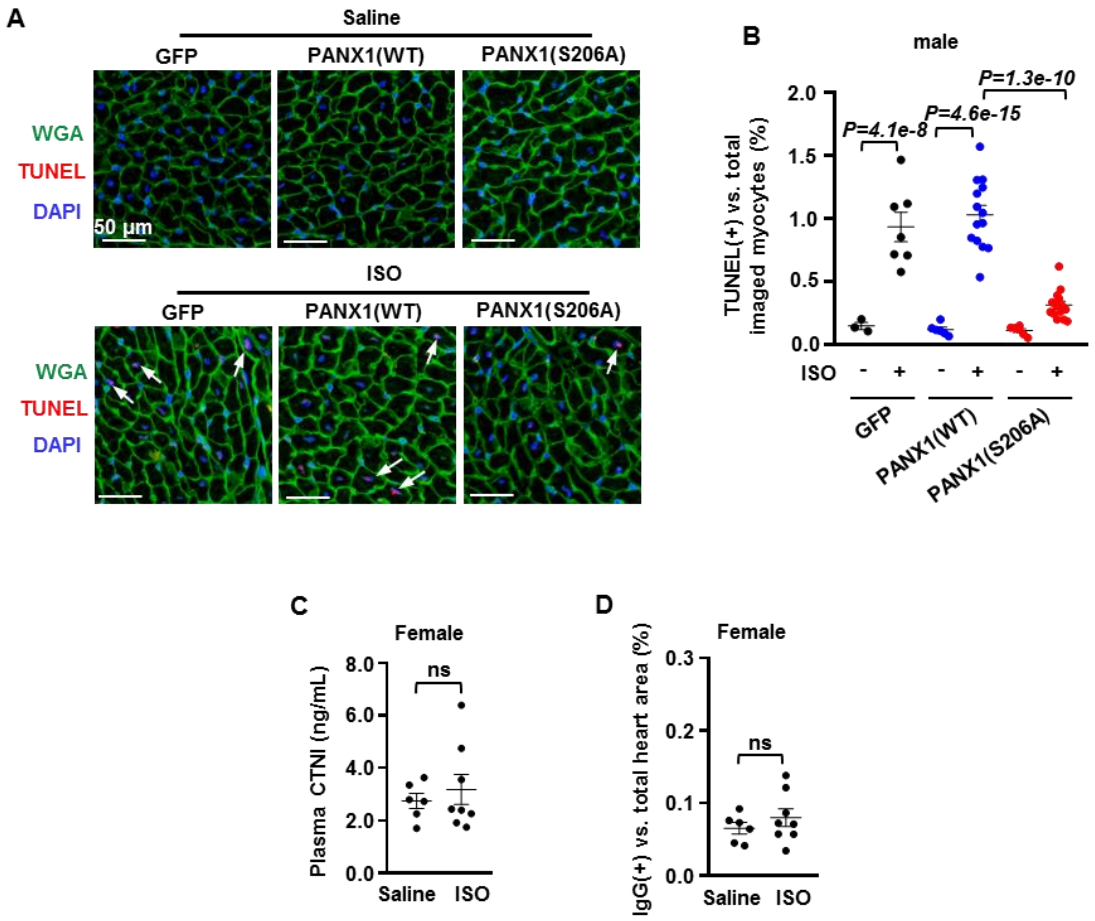

Figure S16. The role of PANX1 phosphorylation at Ser206 in ISO-induced CM apoptosis in male mice; the effect of ISO acute treatment on female mice heart.

A and **B**, Images and quantitative results of TUNEL staining showing PANX1 phosphorylation site mutation significantly reduced ISO-induced CM apoptosis in male mouse hearts. White arrows indicated apoptotic myocardia with TUNEL-positive nuclei. DAPI indicated nuclei, and WGA indicated myocardium in the corresponding fields of heart sections, n=3 (Vehicle/GFP), 7 (ISO/GFP), 6 (Vehicle/PANX1(WT)), 14 (ISO/PANX1(WT)), 6 (Vehicle/PANX1(S206A)), and 14 (ISO/PANX1(S206A)). **C** and **D**, Results of plasma cardiac troponin I (cTNI) levels and myocardial IgG accumulation in female mice. There were no significant changes in plasma cTNI and myocardial IgG staining in female mice with ISO treatment (100 mg/kg, every 8 h twice in 24 h s.c.), n=6 (saline), and 8 (ISO). The representative images were chosen based on their quality and to most accurately reflect the group average across all the available data. Data were presented as mean ± SEM. Data in **Figure S16B** were analyzed by the Kruskal-Wallis test followed by Conover-Iman post-hoc test with Bonferroni corrections for 3 comparisons, **Figures S16C** and **S16D** by the unpaired t-test. The P-value in **Figure S16B** has been adjusted for a predetermined number of multiple comparisons, as specified in the figure, and the raw P-values of **Figures S16C** and **S16D** are reported. P<0.05 was statistically significant. ns: no significant difference.

Figure S17

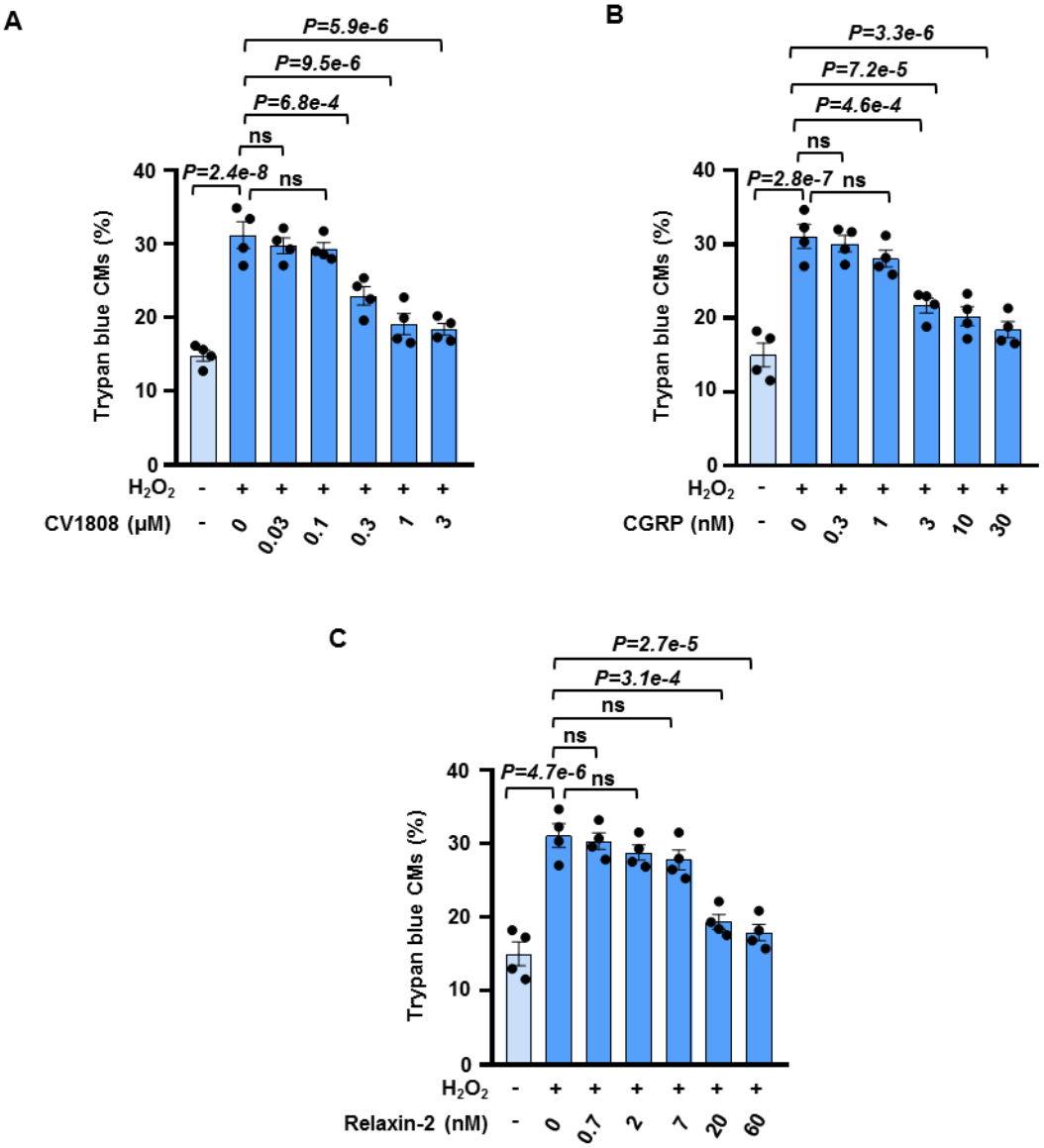
A
P=5.9e-6
P=9.5e-6
P=6.8e-4
ns
P=2.4e-8
ns
Trypan blue CMs (%)
40
30
20
10
0
H2O2 - + + + + + +
CV1808 (μM) - 0 0.03 0.1 0.3 1 3
B
P=3.3e-6
P=7.2e-5
P=4.6e-4
ns
P=2.8e-7
ns
Trypan blue CMs (%)
40
30
20
10
0
H2O2 - + + + + + +
CGRP (nM) - 0 0.3 1 3 10 30
C
P=2.7e-5
P=3.1e-4
ns
ns
P=4.7e-6
ns
Trypan blue CMs (%)
40
30
20
10
0
H2O2 - + + + + + +
Relaxin-2 (nM) - 0 0.7 2 7 20 60

Figure S17. The dose-response studies of the A2AR, CGRPR, or RXFP1 agonist on CM death induced by H_2O_2.

A, Quantitative result of trypan blue exclusion assay showing that A2AR agonist CV1808 protected against CM death induced by H_2O_2 (5 μM for 24 h) in a dose-dependent manner, n=4. **B**, Quantitative result of trypan blue exclusion assay showing that CGRPR agonist CGRP protected against H_2O_2-induced CM death in a dose-dependent manner, n=4. **C**, Quantitative result of trypan blue exclusion assay showing that RXFP1 agonist relaxin-2 protected against H_2O_2-induced CM death in a dose-dependent manner, n=4. Data were presented as mean ± SEM. Data in **Figures S17A-S17C** were analyzed by the Kruskal-Wallis test followed by Conover-Iman post-hoc test with Bonferroni corrections for 6 comparisons. All reported P-values have been adjusted for a predetermined number of multiple comparisons, as specified in the corresponding figures. $P < 0.05$ was statistically significant. ns: no significant difference.

Figure S18

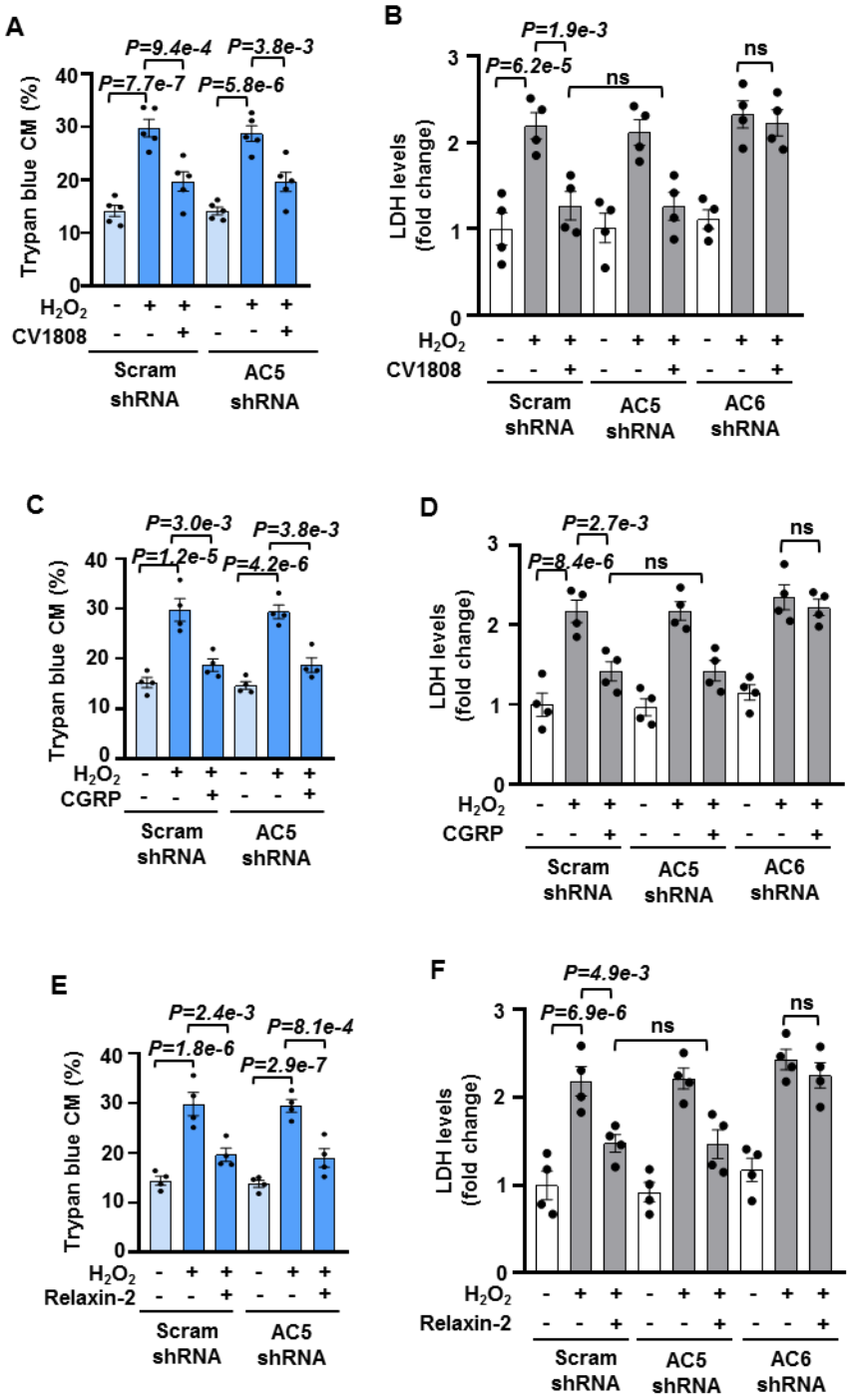
A
P=9.4e-4
P=3.8e-3
P=7.7e-7
P=5.8e-6
Trypan blue CM (%)
H2O2
CV1808
Scram shRNA
AC5 shRNA
B
P=1.9e-3
P=6.2e-5
ns
ns
LDH levels (fold change)
H2O2
CV1808
Scram shRNA
AC5 shRNA
AC6 shRNA
C
P=3.0e-3
P=3.8e-3
P=1.2e-5
P=4.2e-6
Trypan blue CM (%)
H2O2
CGRP
Scram shRNA
AC5 shRNA
D
P=2.7e-3
P=8.4e-6
ns
ns
LDH levels (fold change)
H2O2
CGRP
Scram shRNA
AC5 shRNA
AC6 shRNA
E
P=2.4e-3
P=8.1e-4
P=1.8e-6
P=2.9e-7
Trypan blue CM (%)
H2O2
Relaxin-2
Scram shRNA
AC5 shRNA
F
P=4.9e-3
P=6.9e-6
ns
ns
LDH levels (fold change)
H2O2
Relaxin-2
Scram shRNA
AC5 shRNA
AC6 shRNA

Figure S18. The role of AC5 or AC6 in the protective effect of A2R, CGRPR, or RXFP1 against CM death.

A, **C** and **E,** Quantified results of trypan blue exclusion assay showing that AC5 shRNA did not alter the protective effect of A2R agonist CV1808 (1 μM), CGRPR agonist CGRP (10 nM) or RXFP1 agonist relaxin-2 (20 nM) against CM death induced by H_2O_2 (5 μM for 24 h), n=5 for **A**, 4 for **C** and **E**. **B**, **D** and **F**, Results of LDH leakage showing that AC6 shRNA, but not AC5 shRNA, abolished the protective effect of CV1808, CGRP, or relaxin-2 against CM death, n=4. Data were mean ± SEM. Data in **Figures S18A-S18F** were analyzed by the Kruskal-Wallis test followed by Conover-Iman post-hoc test with Bonferroni corrections for 4 comparisons. All reported P-values have been adjusted for a predetermined number of multiple comparisons, as specified in the corresponding figures. P <0.05 was statistically significant. ns: no significant difference.

Figure S19

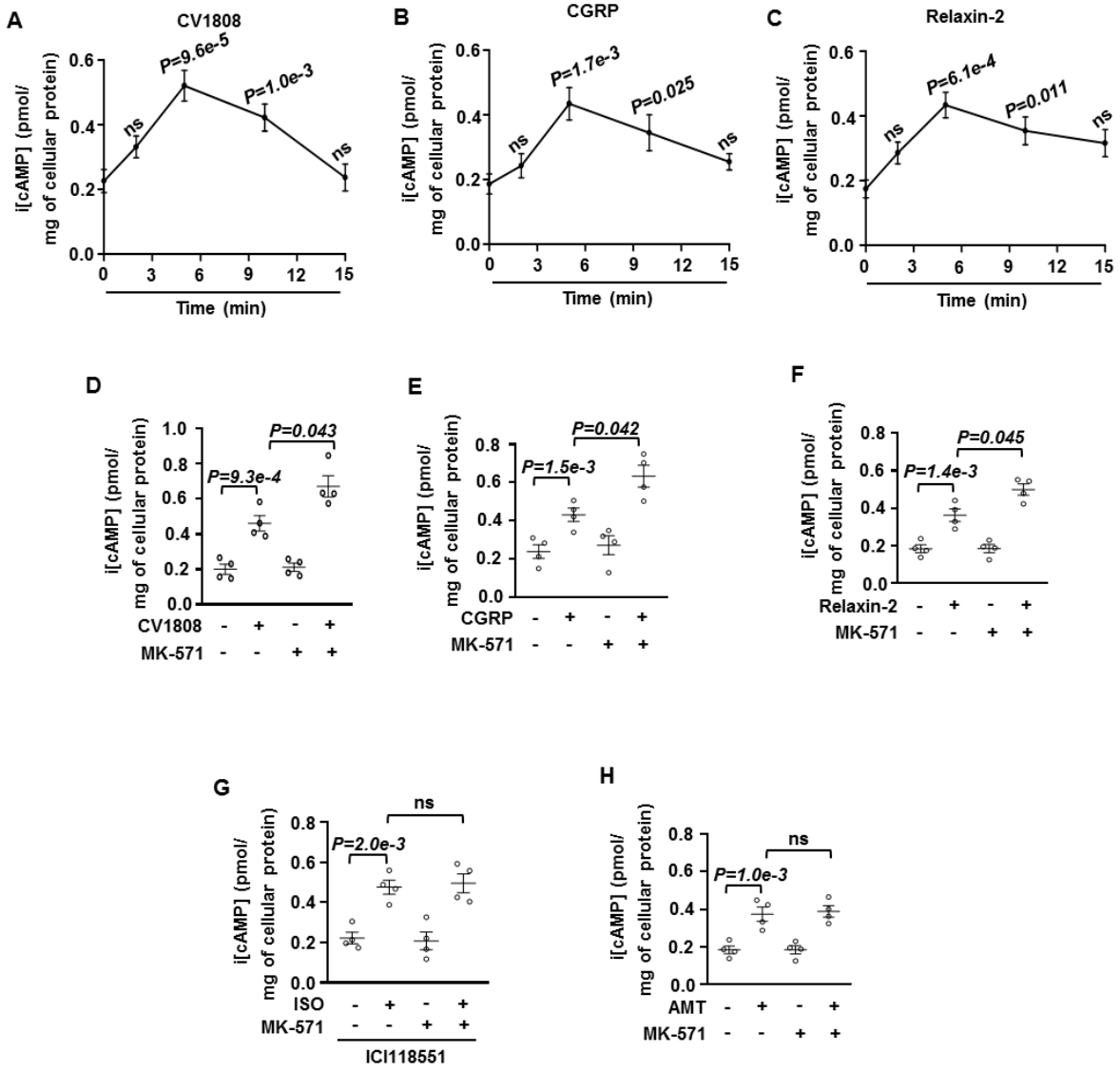
A
CV1808
i[cAMP] (pmol/ mg of cellular protein)
P=9.6e-5
P=1.0e-3
ns
ns
Time (min)
B
CGRP
P=1.7e-3
P=0.025
C
Relaxin-2
P=6.1e-4
P=0.011
D
P=9.3e-4
P=0.043
CV1808
MK-571
E
P=1.5e-3
P=0.042
CGRP
F
P=1.4e-3
P=0.045
Relaxin-2
G
P=2.0e-3
ISO
ICI118551
H
P=1.0e-3
AMT

Figure S19. Time course of A2R-, CGRPR- or RXFP1-induced i[cAMP] in CMs; the role of MRP in various GsPCR-induced i[cAMP].

A-C, Time course of i[cAMP] levels induced by A2R agonist CV1808 (1 μM), CGRPR agonist CGRP (10 nM), or RXFP1 agonist relaxin-2 (20 nM) as indicated. CV1808-, CGRP- or relaxin-2-induced i[cAMP] peaked at 5 min, n=4. The statistics were performed by comparing to the 0-min time point. **D-F**, Results of i[cAMP] levels showing that pan MRP blocker MK-571 (10 μM) enhanced CV1808-, CGRP- or relaxin-2- induced elevation of i[cAMP]. It implicates that CV1808-, CGRP- or relaxin-2-induced i[cAMP] could efflux via MRPs, n=4. **G** and **H**, Results of i[cAMP] levels showing that MK-571 had no significant effect on elevation of i[cAMP] induced by βAR agonist ISO (10 μM for 5 min) or H2R agonist AMT (10 μM for 5 min). It implies that ISO- or AMT-induced i[cAMP] could not efflux via MRPs, n=4. Data were mean ± SEM. Data in **Figures S19A-S19C** were analyzed by the Kruskal-Wallis test followed by Conover-Iman post-hoc test with Bonferroni corrections for 4 comparisons, and **Figures S19D-S19H** by the two-way ART ANOVA with Bonferroni post-hoc test corrections for 2 comparisons. All reported P-values have been adjusted for a predetermined number of multiple comparisons, as specified in the corresponding figures. $P < 0.05$ was statistically significant. ns: no significant difference.

Figure S20

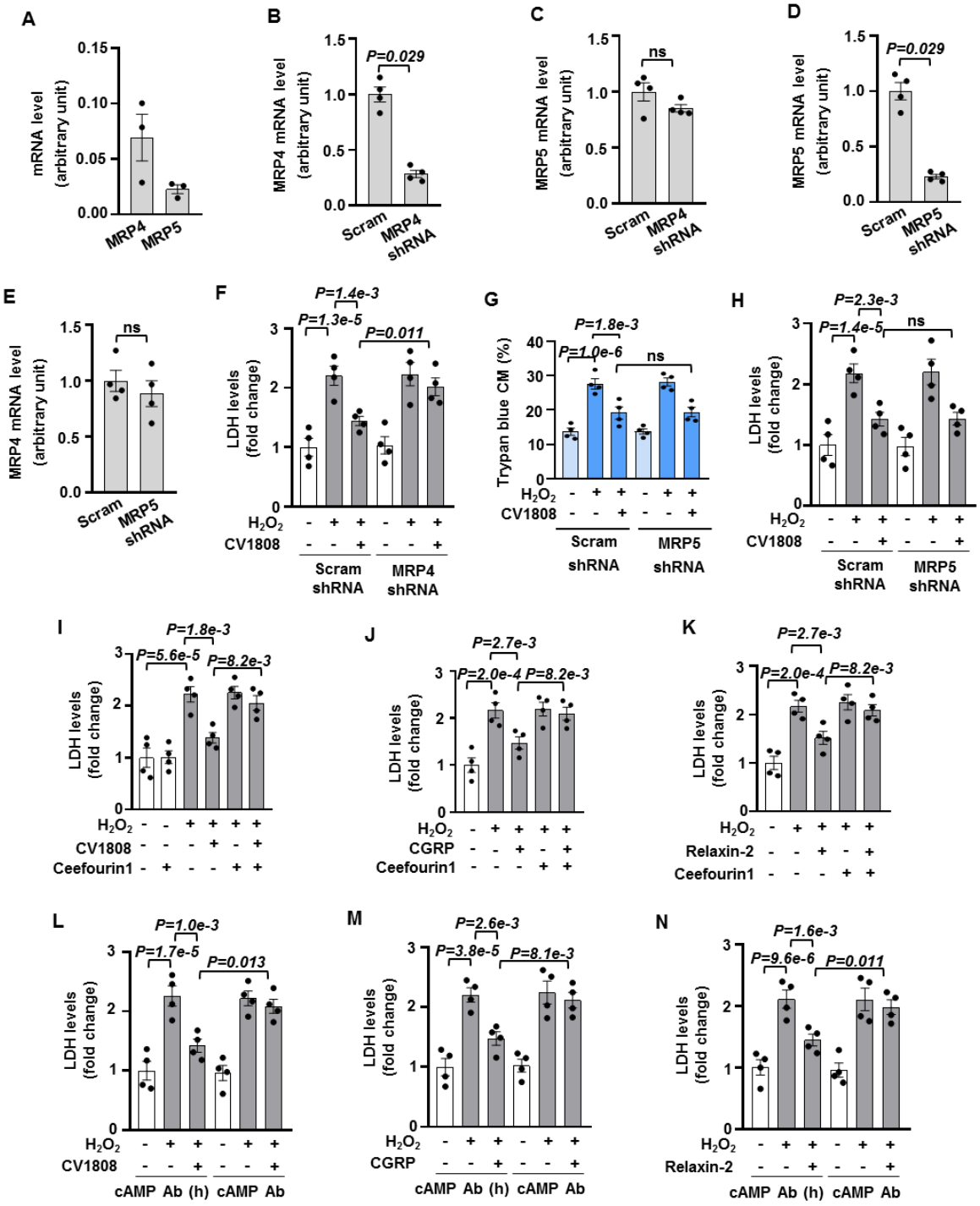
A
mRNA level (arbitrary unit)
MRP4
MRP5
B
MRP4 mRNA level (arbitrary unit)
P=0.029
Scram
MRP4 shRNA
C
MRP5 mRNA level (arbitrary unit)
ns
Scram
MRP4 shRNA
D
MRP5 mRNA level (arbitrary unit)
P=0.029
Scram
MRP5 shRNA
E
MRP4 mRNA level (arbitrary unit)
ns
Scram
MRP5 shRNA
F
LDH levels (fold change)
P=1.4e-3
P=1.3e-5
P=0.011
H2O2
CV1808
Scram shRNA
MRP4 shRNA
G
Trypan blue CM (%)
P=1.8e-3
P=1.0e-6
ns
H2O2
CV1808
Scram shRNA
MRP5 shRNA
H
LDH levels (fold change)
P=2.3e-3
P=1.4e-5
ns
H2O2
CV1808
Scram shRNA
MRP5 shRNA
I
LDH levels (fold change)
P=1.8e-3
P=5.6e-5
P=8.2e-3
H2O2
CV1808
Ceefourin1
J
LDH levels (fold change)
P=2.7e-3
P=2.0e-4
P=8.2e-3
H2O2
CGRP
Ceefourin1
K
LDH levels (fold change)
P=2.7e-3
P=2.0e-4
P=8.2e-3
H2O2
Relaxin-2
Ceefourin1
L
LDH levels (fold change)
P=1.0e-3
P=1.7e-5
P=0.013
H2O2
CV1808
cAMP
Ab (h)
cAMP
Ab
M
LDH levels (fold change)
P=2.6e-3
P=3.8e-5
P=8.1e-3
H2O2
CGRP
cAMP
Ab (h)
cAMP
Ab
N
LDH levels (fold change)
P=1.6e-3
P=9.6e-6
P=0.011
H2O2
Relaxin-2
cAMP
Ab (h)
cAMP
Ab

Figure S20. The role of MRP-induced e[cAMP] in the protective effect of A2R, CGRPR, and RXFP1 against CM death using MRP4 or MRP5 shRNA, MRP4 inhibitor or cAMP antibody. **A**, RT-qPCR results showing relative mRNA levels of MRP4 and MRP5 in adult mouse CMs, n=3. Data were normalized by the housekeeping gene GAPDH. **B** and **C**, RT-qPCR results showing mRNA levels of MRP4 or MRP5 in CMs treated with MRP4 shRNA via lentivirus. MRP4 shRNA largely reduced MRP4 expression but did not significantly affect MRP5 expression. These results demonstrated the efficiency and specificity of MRP4 gene knocking down (KD) , n=4. Data were normalized by the housekeeping gene GAPDH. The result was presented as the fold change of the control group average. **D** and **E**, RT-qPCR results showing mRNA levels of MRP4 or MRP5 in CMs treated with MRP5 shRNA via lentivirus. MRP5 shRNA largely reduced MRP5 expression but did not significantly affect MRP4 expression. These results demonstrated the efficiency and specificity of MRP5 KD, n=4. Data were normalized by the housekeeping gene GAPDH. The result was presented as the fold change of the control group average. **F**, Results of LDH leakage showing that MRP4 shRNA abolished the protective effect of A2R agonist CV1808 (1 μM) against CM death induced by H_2O_2 (5 μM for 24 h), n=4. **G** and **H**, Results of trypan blue exclusion assay and LDH leakage showing that MRP5 shRNA did not significantly affect the protective effect of CV1808, n=4. **I-K**, Results of LDH leakage showing that MRP4 inhibitor ceefourin1 (20 μM) abolished the effect of CV1808, CGRPR agonist CGRP (10 nM), or RXFP1 agonist relaxin-2 (20 nM) on CM viability, n=4. **L-N**, Results of LDH leakage showing that the cAMP antibody (0.25 μg/mL), but not the heat-inactivated one, blocked the effect of CV1808, CGRP, or relaxin-2 on CM viability, n=4. Data were mean ± SEM. Data in **Figures S20F-S20N** were analyzed by the Kruskal-Wallis test followed by Conover-Iman post-hoc test with Bonferroni corrections for 3 comparisons, and **Figures S20B-S20E** by the Mann-Whitney test. All reported P-values have been adjusted for a predetermined number of multiple comparisons, as specified in the corresponding figures, except in **Figures S20B-S20E,** where raw P-values are reported. $P < 0.05$ was statistically significant. ns: no significant difference.

Figure S21

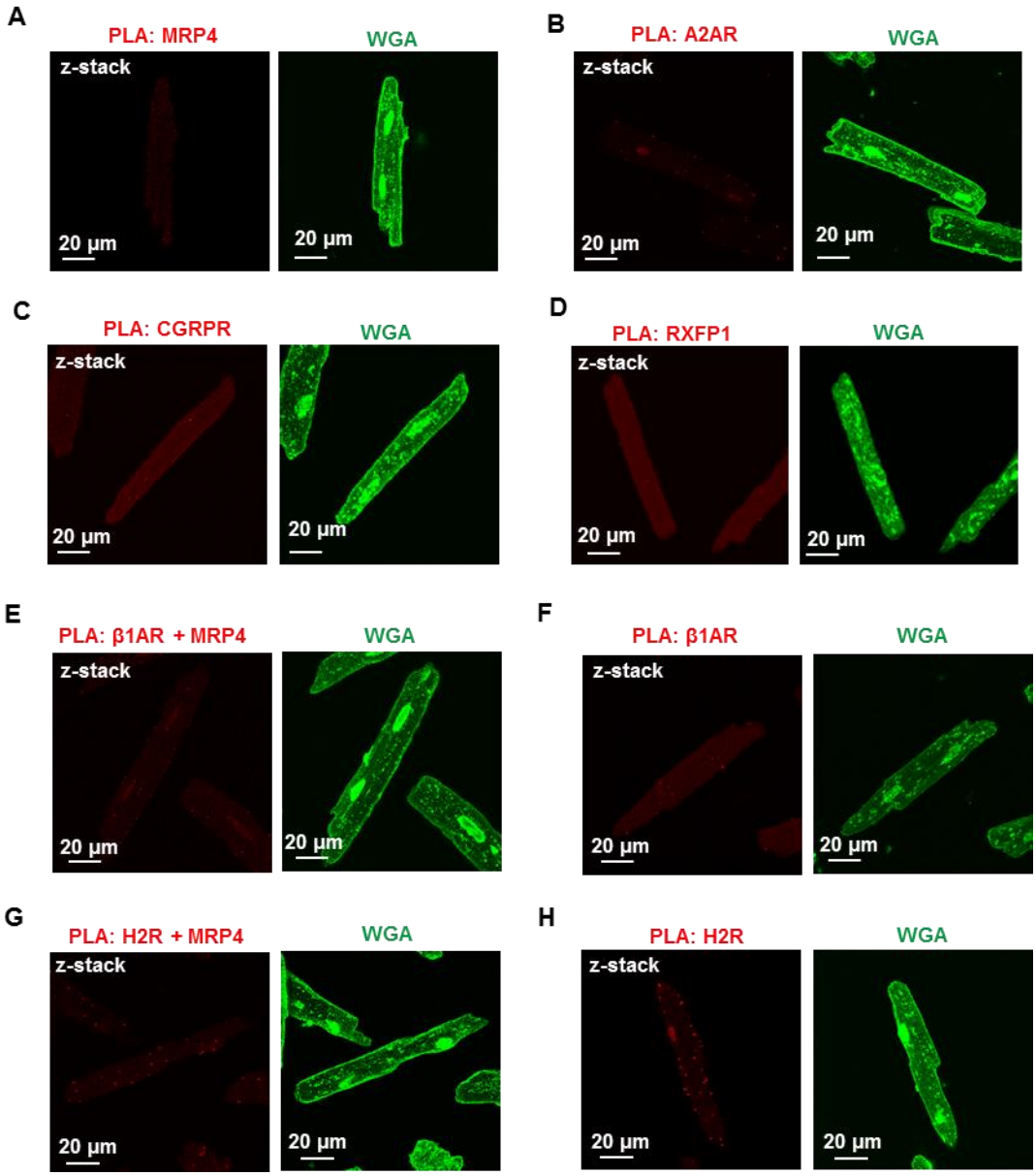
A
PLA: MRP4
WGA
z-stack
20 µm
20 µm
B
PLA: A2AR
WGA
z-stack
20 µm
20 µm
C
PLA: CGRPR
WGA
z-stack
20 µm
20 µm
D
PLA: RXFP1
WGA
z-stack
20 µm
20 µm
E
PLA: β1AR + MRP4
WGA
z-stack
20 µm
20 µm
F
PLA: β1AR
WGA
z-stack
20 µm
20 µm
G
PLA: H2R + MRP4
WGA
z-stack
20 µm
20 µm
H
PLA: H2R
WGA
z-stack
20 µm
20 µm

Figure S21. PLA negative controls for MRP4, A2AR, CGRPR, RXFP1, β1AR or H2R in CMs; PLA of MRP4 with β1AR or H2R in CMs.

A-D, PLA results showing negative controls performed with MRP4, A2AR, CGRPR, or RXFP1 antibody alone in CMs. WGA images showing CMs in the corresponding fields. There was no significant PLA signal detected in negative controls. **E** and **G**, Images of PLA performed by MRP4 plus β1AR or H2R antibodies together in CMs. WGA images showing CMs in the corresponding fields. No significant PLA positive signals were detected between MRP4 and β1AR or H2R, indicating no apparent interaction between MRP4 and β1AR or H2R detected. **F** and **H**, PLA results showing negative controls performed with β1AR or H2R antibody alone in CMs. WGA images showing CMs in the corresponding fields. There was no significant PLA signal detected in negative controls.

Figure S22

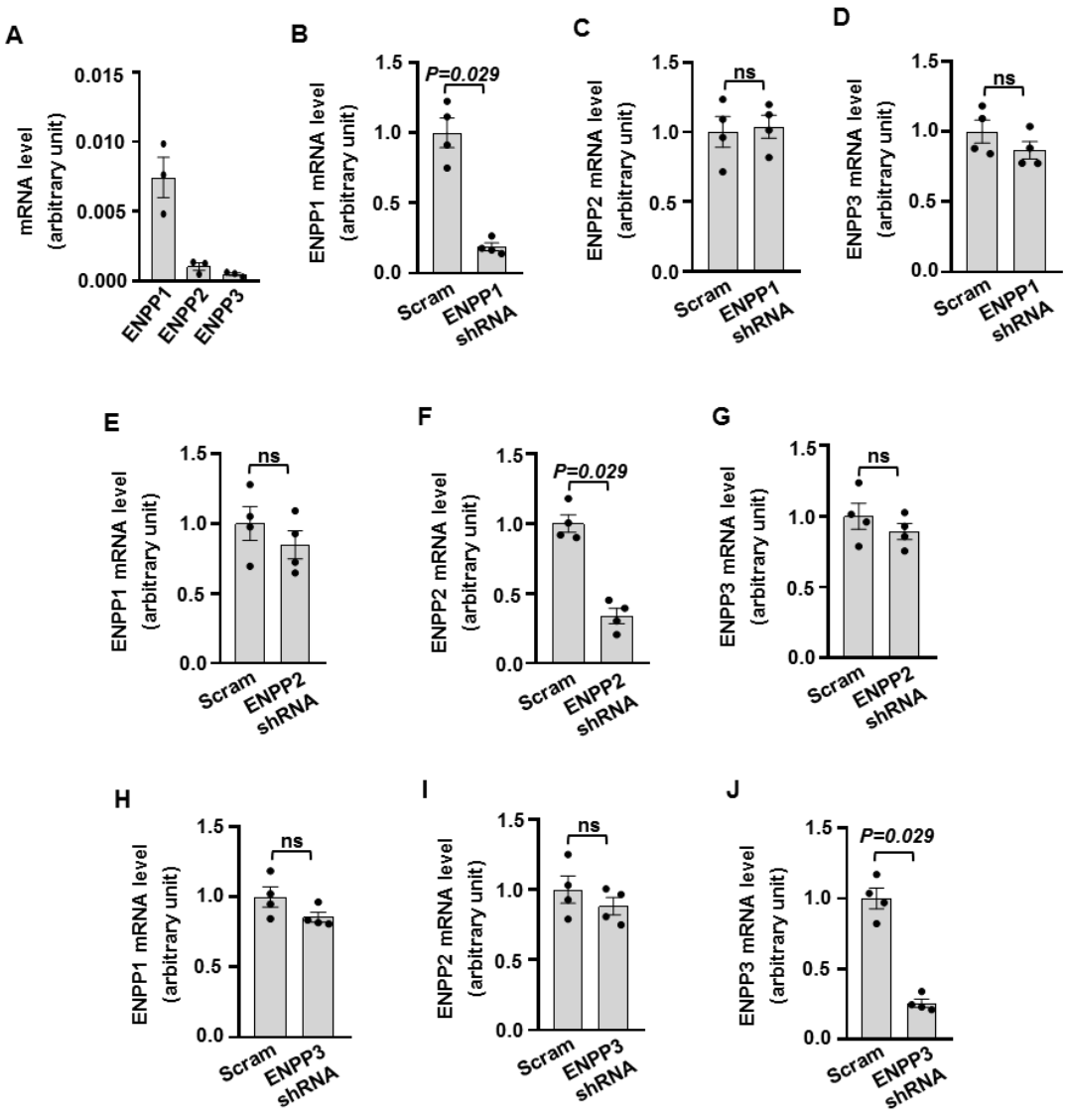
A
mRNA level (arbitrary unit)
0.015
0.010
0.005
0.000
ENPP1
ENPP2
ENPP3
B
ENPP1 mRNA level (arbitrary unit)
P=0.029
Scram
ENPP1 shRNA
C
ENPP2 mRNA level (arbitrary unit)
ns
Scram
ENPP1 shRNA
D
ENPP3 mRNA level (arbitrary unit)
ns
Scram
ENPP1 shRNA
E
ENPP1 mRNA level (arbitrary unit)
ns
Scram
ENPP2 shRNA
F
ENPP2 mRNA level (arbitrary unit)
P=0.029
Scram
ENPP2 shRNA
G
ENPP3 mRNA level (arbitrary unit)
ns
Scram
ENPP2 shRNA
H
ENPP1 mRNA level (arbitrary unit)
ns
Scram
ENPP3 shRNA
I
ENPP2 mRNA level (arbitrary unit)
ns
Scram
ENPP3 shRNA
J
ENPP3 mRNA level (arbitrary unit)
P=0.029
Scram
ENPP3 shRNA

Figure S22. ENPP1, ENPP2, or ENPP3 shRNA efficiency and specificity.
A, RT-qPCR results showing relative mRNA expression levels of ENPP1, 2, and 3 in adult mouse CMs, n=3. Data were normalized by the housekeeping gene GAPDH. **B-D**, RT-qPCR results showing ENPP1, ENPP2, or ENPP3 mRNA in CMs treated with ENPP1 shRNA via lentivirus. ENPP1 shRNA largely reduced ENPP1 expression but had no significant effect on ENPP2 or ENPP3 expression. These results demonstrated the efficiency and specificity of ENPP1 gene KD, n=4. **E**-**G**, RT-qPCR results showing ENPP1, ENPP2, or ENPP3 mRNA in CMs treated with ENPP2 shRNA via lentivirus. ENPP2 shRNA largely reduced ENPP2 expression but did not significantly affect ENPP1 or ENPP3 expression. These results demonstrated the efficiency and specificity of ENPP2 gene KD, n=4. **H**-**J**, RT-qPCR results showing mRNA levels of ENPP1, ENPP2, or ENPP3 in CMs treated with ENPP3 shRNA via lentivirus. ENPP3 shRNA largely reduced ENPP3 expression but did not significantly affect ENPP1 or ENPP2 expression. These results demonstrated the efficiency and specificity of ENPP3 gene KD, n=4. Data for quantification gene expression were normalized by the housekeeping gene GAPDH. The result was presented as the fold change of the control group average. Data were mean ± SEM. Data in **Figures S22B-S22J** were analyzed by the Mann-Whitney test. All raw P-values are reported. $P < 0.05$ was statistically significant. ns: no significant difference.

Figure S23

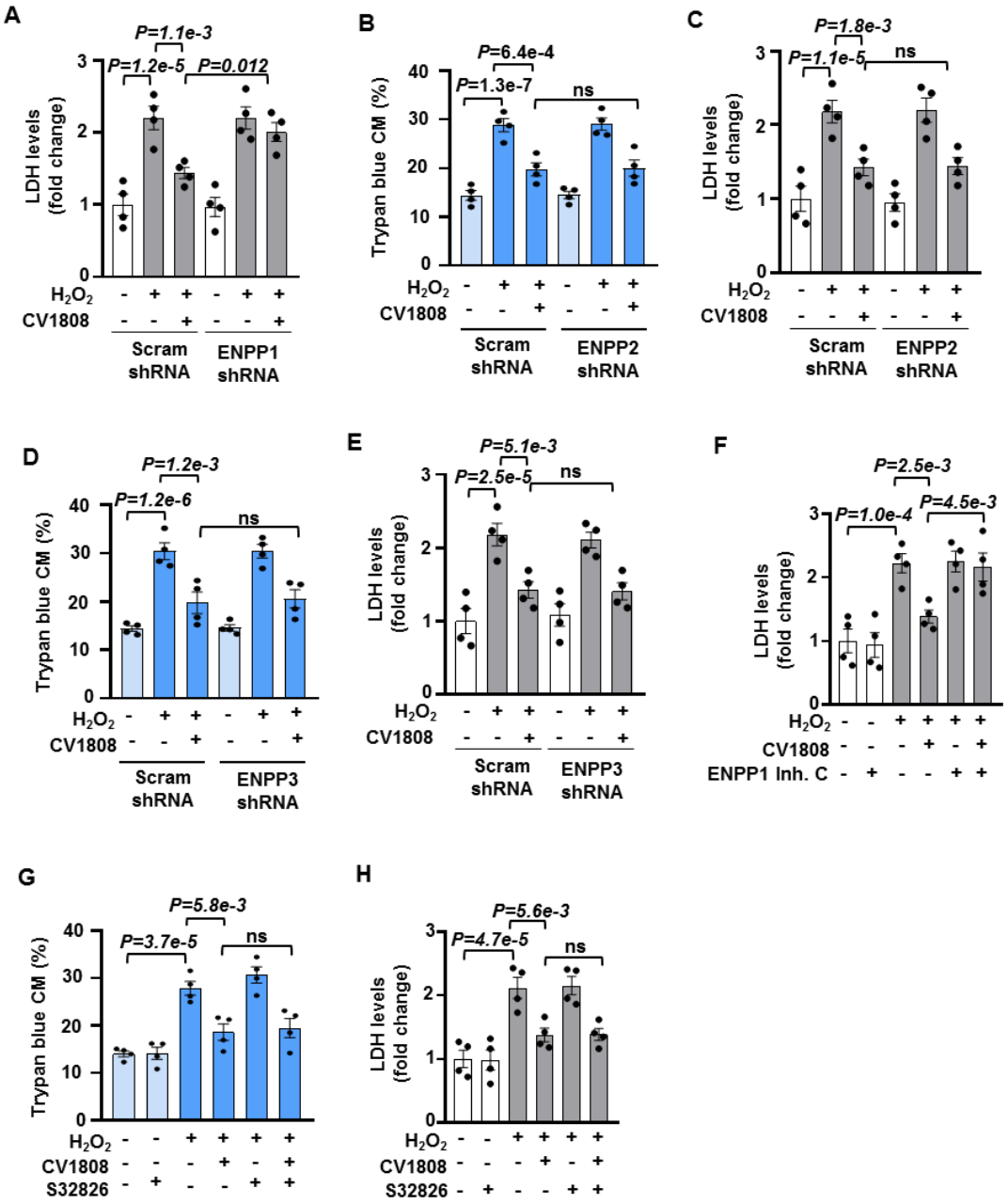
A
P=1.1e-3
P=1.2e-5
P=0.012
LDH levels (fold change)
H2O2
CV1808
Scram shRNA
ENPP1 shRNA
B
P=6.4e-4
P=1.3e-7
ns
Trypan blue CM (%)
Scram shRNA
ENPP2 shRNA
C
P=1.8e-3
P=1.1e-5
ns
LDH levels (fold change)
Scram shRNA
ENPP2 shRNA
D
P=1.2e-3
P=1.2e-6
ns
Trypan blue CM (%)
Scram shRNA
ENPP3 shRNA
E
P=5.1e-3
P=2.5e-5
ns
LDH levels (fold change)
Scram shRNA
ENPP3 shRNA
F
P=2.5e-3
P=1.0e-4
P=4.5e-3
LDH levels (fold change)
ENPP1 Inh. C
G
P=5.8e-3
P=3.7e-5
ns
Trypan blue CM (%)
S32826
H
P=5.6e-3
P=4.7e-5
ns
LDH levels (fold change)
S32826

Figure S23. The role of ENPP1, 2, or 3 in the protective effect of A2R against CM death. **A**, Results of LDH leakage showing that ENNP1 shRNA significantly abolished the effect of A2R agonist CV1808 (1 μM) on LDH leakage induced by H_2O_2 (5 μM for 24 h), n=4. **B** and **C**, Results of trypan blue exclusion assay and LDH leakage showing that ENNP2 shRNA did not alter the protective effect of CV1808 against H_2O_2-induced CM death and LDH leakage, n=4. **D** and **E**, Results of trypan blue exclusion assay and LDH leakage showing that ENNP3 shRNA did not alter the effect of CV1808 on CM viability, n=4. **F**, Results of LDH leakage showing that ENPP1 inhibitor (ENPP1 inhibitor C, 10 μM) significantly abolished the protective effect of CV1808 against H_2O_2-induced LDH leakage, n=4. **G** and **H**, Results of trypan blue exclusion assay and LDH leakage show that ENPP2 inhibitor S32826 (10 μM) did not significantly affect the protective effect of CV1808 against H_2O_2-induced CM death and LDH leakage, n=4. Data were mean ± SEM. Data in **Figures S23A-S23H** were analyzed by the Kruskal-Wallis test followed by Conover-Iman post-hoc test with Bonferroni corrections for 3 comparisons. All reported P-values have been adjusted for a predetermined number of multiple comparisons, as specified in the corresponding figures. P <0.05 was statistically significant. ns: no significant difference.

Figure S24

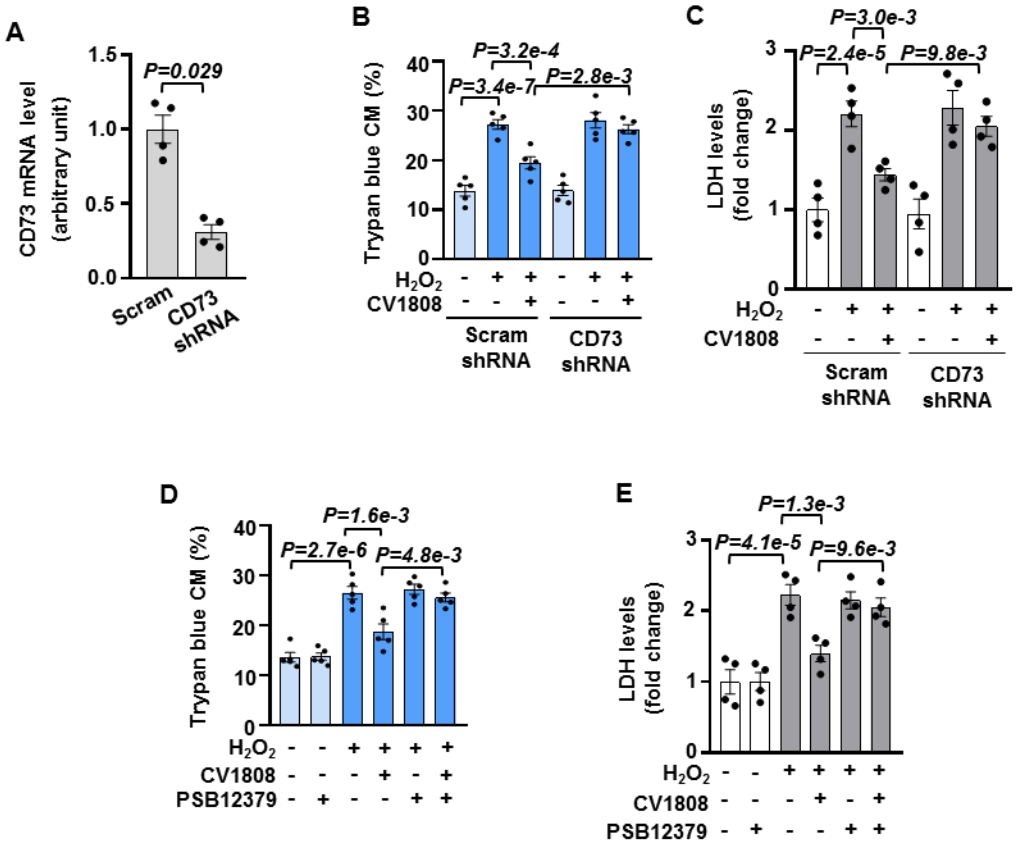

Figure S24. The role of CD73 in the protective effect of A2R against CM death.
A, RT-qPCR results showing mRNA levels of CD73 in CMs treated with CD73 shRNA via lentivirus. CD73 shRNA largely reduced CD73 expression, n=4. Data were normalized by house keeping gene GAPDH. The result was presented as the fold change of the control group average. **B-E**, Results of trypan blue exclusion assay and LDH leakage showing that CD73 shRNA or CD73 inhibitor PSB12379 (10 μM) abolished the protective effect of CV1808 on CM survival, n=5 for **B** and **D**, 4 for **C** and **E**. Data were mean ± SEM. Data in **Figures S24B-S24E** were analyzed by the Kruskal-Wallis test followed by Conover-Iman post-hoc test with Bonferroni corrections for 3 comparisons, and **Figure S24A** by the Mann-Whitney test. All reported P-values have been adjusted for a predetermined number of multiple comparisons, as specified in the corresponding figures, except in **Figure S24A** where raw P-value is reported. P <0.05 was statistically significant.

Figure S25

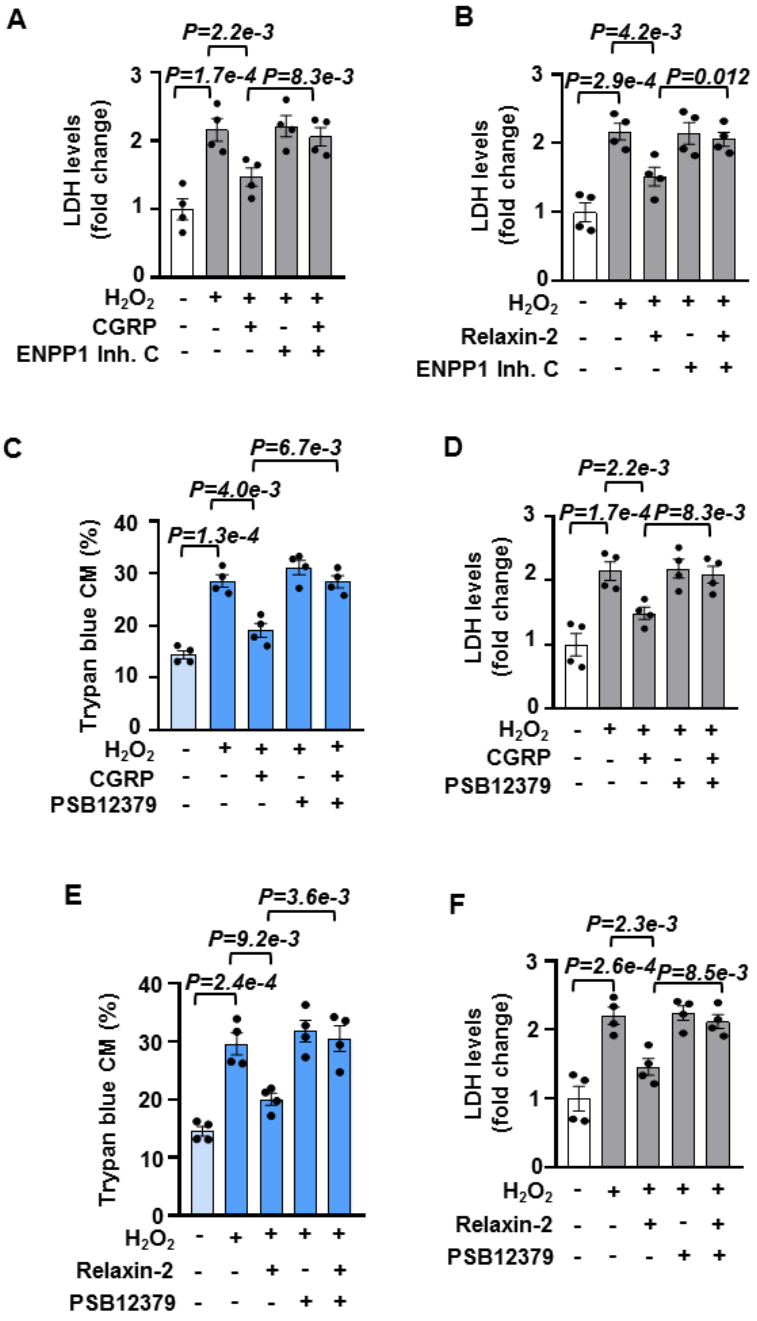
A
P=2.2e-3
P=1.7e-4
P=8.3e-3
LDH levels (fold change)
H2O2
CGRP
ENPP1 Inh. C
B
P=4.2e-3
P=2.9e-4
P=0.012
LDH levels (fold change)
H2O2
Relaxin-2
ENPP1 Inh. C
C
P=6.7e-3
P=4.0e-3
P=1.3e-4
Trypan blue CM (%)
H2O2
CGRP
PSB12379
D
P=2.2e-3
P=1.7e-4
P=8.3e-3
LDH levels (fold change)
H2O2
CGRP
PSB12379
E
P=3.6e-3
P=9.2e-3
P=2.4e-4
Trypan blue CM (%)
H2O2
Relaxin-2
PSB12379
F
P=2.3e-3
P=2.6e-4
P=8.5e-3
LDH levels (fold change)
H2O2
Relaxin-2
PSB12379

Figure S25. The role of ENPP1 and CD73 in the protective effect of CGRPR or RXFP1 against CM death.

A and **B**, Results of LDH leakage showing that ENPP1 inhibitor (ENPP1 inhibitor C, 10 μM) significantly abolished the protective effect of CGRPR agonist CGRP (10 nM) or RXFP1 agonist relaxin-2 (20 nM) against CM death induced by H_2O_2 (10 μM for 24 h), n=4. **C-F**, Results of trypan blue exclusion assay and LDH leakage showing that CD37 inhibitor PSB12379 (10 μM) inhibited the protective effect of CGRP or relaxin-2 on CM survival, n=4. Data were mean ± SEM. Data in **Figures S25A-S25F** were analyzed by the Kruskal-Wallis test followed by Conover-Iman post-hoc test with Bonferroni corrections for 3 comparisons. All reported P-values have been adjusted for a predetermined number of multiple comparisons, as specified in the corresponding figures. P <0.05 was statistically significant. ns: no significant difference.

Figure S26

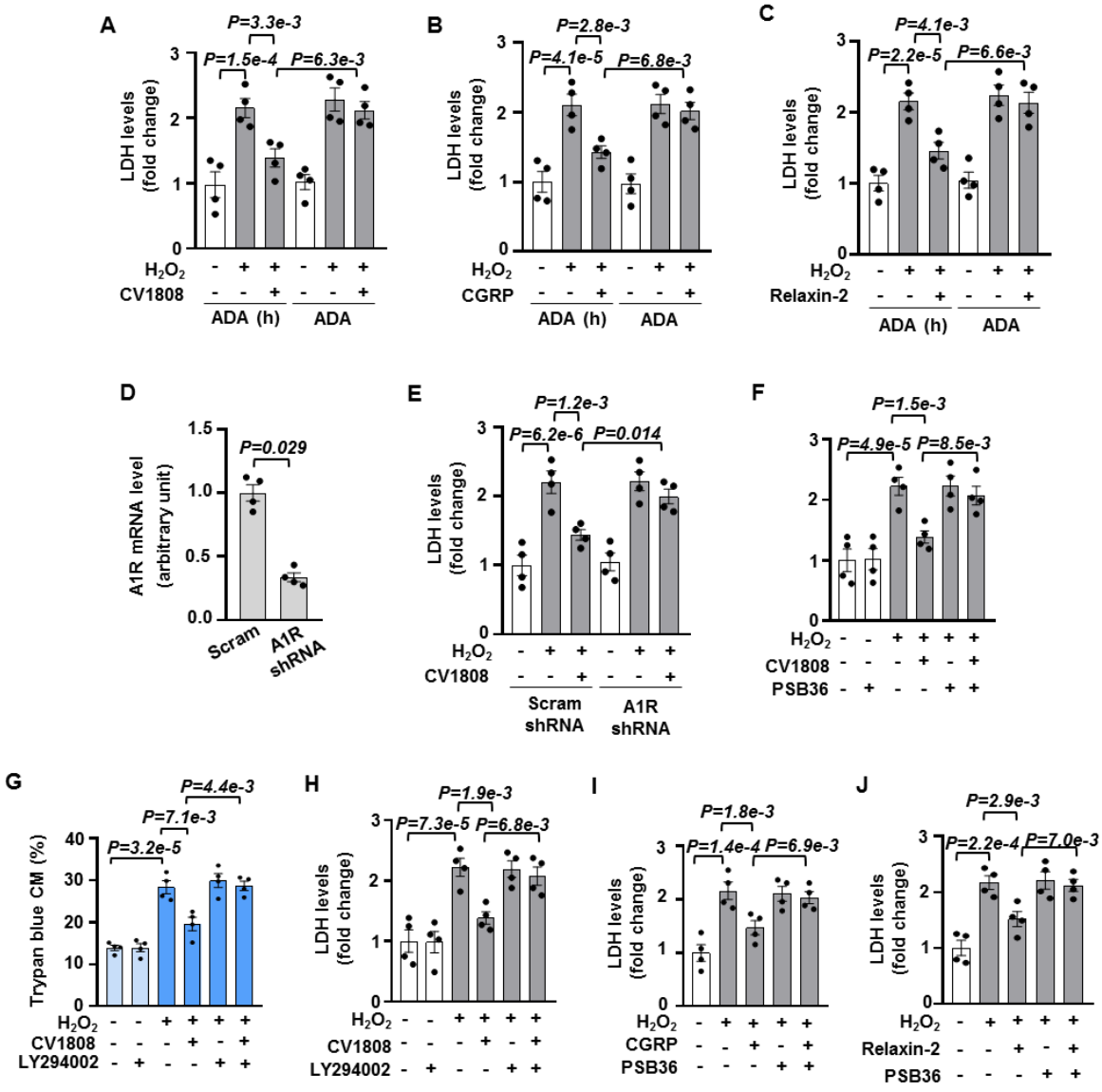
A
P=3.3e-3
P=1.5e-4
P=6.3e-3
LDH levels (fold change)
H2O2
CV1808
ADA (h)
ADA
B
P=2.8e-3
P=4.1e-5
P=6.8e-3
CGRP
C
P=4.1e-3
P=2.2e-5
P=6.6e-3
Relaxin-2
D
P=0.029
A1R mRNA level (arbitrary unit)
Scram
A1R shRNA
E
P=1.2e-3
P=6.2e-6
P=0.014
Scram shRNA
A1R shRNA
F
P=1.5e-3
P=4.9e-5
P=8.5e-3
PSB36
G
P=4.4e-3
P=7.1e-3
P=3.2e-5
Trypan blue CM (%)
LY294002
H
P=1.9e-3
P=7.3e-5
P=6.8e-3
I
P=1.8e-3
P=1.4e-4
P=6.9e-3
J
P=2.9e-3
P=2.2e-4
P=7.0e-3

Figure S26. The role of e[ADO], A1R, or PI3K in the protective effect of pro-survival GsPCRs against CM death.

A-C, Results of LDH leakage showing that depleting e[ADO] with active ADA (1.2 U/mL) significantly inhibited the protective effect of A2R agonist CV1808 (1 μM), CGRPR agonist CGRP (10 nM) or RXFP1 agonist (20 nM) against LDH leakage induced by H_2O_2 (5 μM for 24 h). The heat-inactivated ADA was used as a negative control, n=4. **D**, RT-qPCR results showing mRNA levels of A1R in CMs treated with A1R shRNA via lentivirus. A1R shRNA largely reduced A1R expression, n=4. Data were normalized by the housekeeping gene GAPDH. The result was presented as the fold change of the control group average. **E** and **F**, Results of LDH leakage showing that A1R shRNA or A1R antagonist PSB36 (10 nM) significantly abolished the protective effect of CV1808 on CM survival, n=4. **G** and **H**, Results of trypan blue exclusion assay and LDH leakage showing that PI3K inhibitor LY284002 (10 μM) significantly abolished the protective effect of CV1808 against H_2O_2-induced CM death and LDH leakage, n=4. **I** and **J**, Results of LDH leakage showing that PSB36 abolished the protective effect of CGRP or relaxin-2 on CM survival, n=4. Data were mean ± SEM. Data in **Figures S26A-S26C** and **S26E-S26J** were analyzed by the Kruskal-Wallis test followed by Conover-Iman post-hoc test with Bonferroni corrections for 3 comparisons, and **Figure S26D** by the Mann-Whitney test. All reported P-values have been adjusted for a predetermined number of multiple comparisons, as specified in the corresponding figures, except in **Figure S26D** where raw P-value is reported. $P < 0.05$ was statistically significant.

Figure S27

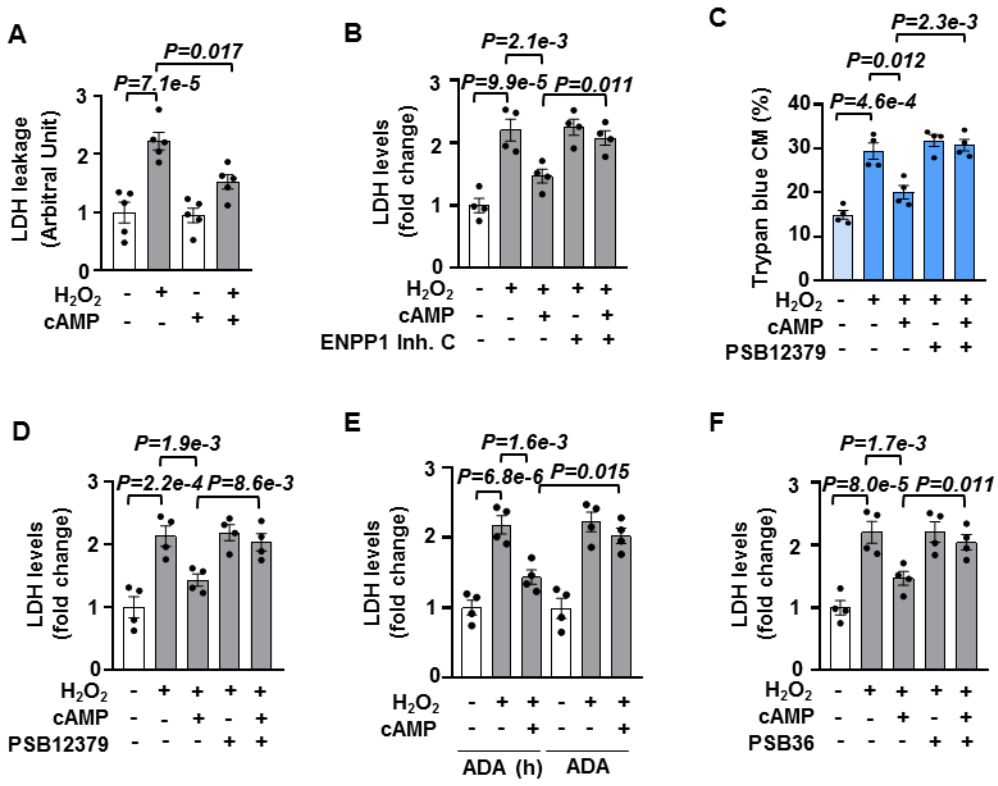

Figure S27. The role of ENPP1, CD73, e[ADO], and A1R in the protective effect of e[cAMP] on CM survival.

A, Results of LDH leakage showing that exogenous membrane impermeable cAMP (cAMP, 10 μM) largely inhibited LDH leakage induced by H_2O_2 (5 μM for 24 h), n=5. **B**, Results of LDH leakage showing that ENPP1 inhibitor (ENPP1 inhibitor C, 10 μM) significantly abolished the protective effect of cAMP on CM survival, n=4. **C** and **D**, Results of trypan blue exclusion assay and LDH leakage showing that CD73 inhibitor PSB12379 (10 μM) significantly abolished the protective effect of cAMP against CM death and LDH leakage induced by H_2O_2 (5 μM for 24 h), n=4. **E**, Result of LDH leakage showing that depleting e[ADO] with active ADA (1.2 U/mL) significantly inhibited the protective effect of cAMP on CM survival. The heat-inactivated ADA was used as a negative control, n=4. **F**, Results of LDH leakage showing that A1R antagonist PSB36 (10 nM) significantly inhibited the protective effect of cAMP on CM survival, n=4. Data were mean ± SEM. Data in **Figures S27B-S27F** were analyzed by the Kruskal-Wallis test followed by Conover-Iman post-hoc test with Bonferroni corrections for 3 comparisons, and **Figure S27A** by the two-way ART ANOVA with Bonferroni post-hoc test corrections for 2 comparisons. All reported P-values have been adjusted for a predetermined number of multiple comparisons, as specified in the corresponding figures. P <0.05 was statistically significant.

Figure S28

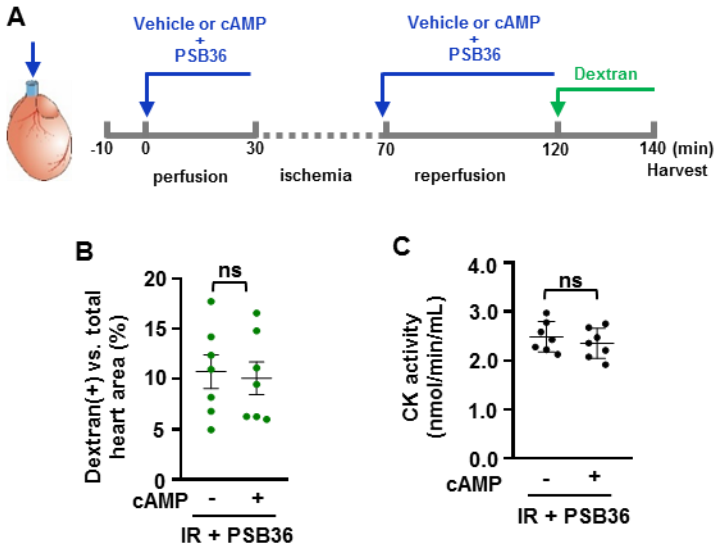

Figure S28. The role of A1R in the protective effect of exogenous cAMP against myocardial IR injury in *ex vivo* hearts.

A, Diagram of the *ex vivo* experiment design: Isolated mouse hearts were connected to a Langendorff perfusion system and subjected to 30 min equilibration, 40 min global ischemia with no flow, followed by 50 min reperfusion with A1R antagonist PSB36 (20 nM) or PSB36 plus cAMP (20 μM). **B**, Quantified results of myocardial FITC-dextran accumulation (an indicator of cardiac injury) showing that PSB36 largely abrogated the protective effect of exogenous membrane impermeable cAMP against IR-induced myocardial injury *ex vivo*, n=7. **C**, Results of CK activity in coronary outflow showing that PSB36 significantly inhibited the protective effect of cAMP reducing CK activity from mouse hearts with *ex vivo* IR, n=7. Data were presented as mean ± SEM. Data in **Figures S28B** and **S28C** were analyzed by the unpaired t-test. All raw P-values are reported. P <0.05 was statistically significant. ns: no significant difference.

Figure S29

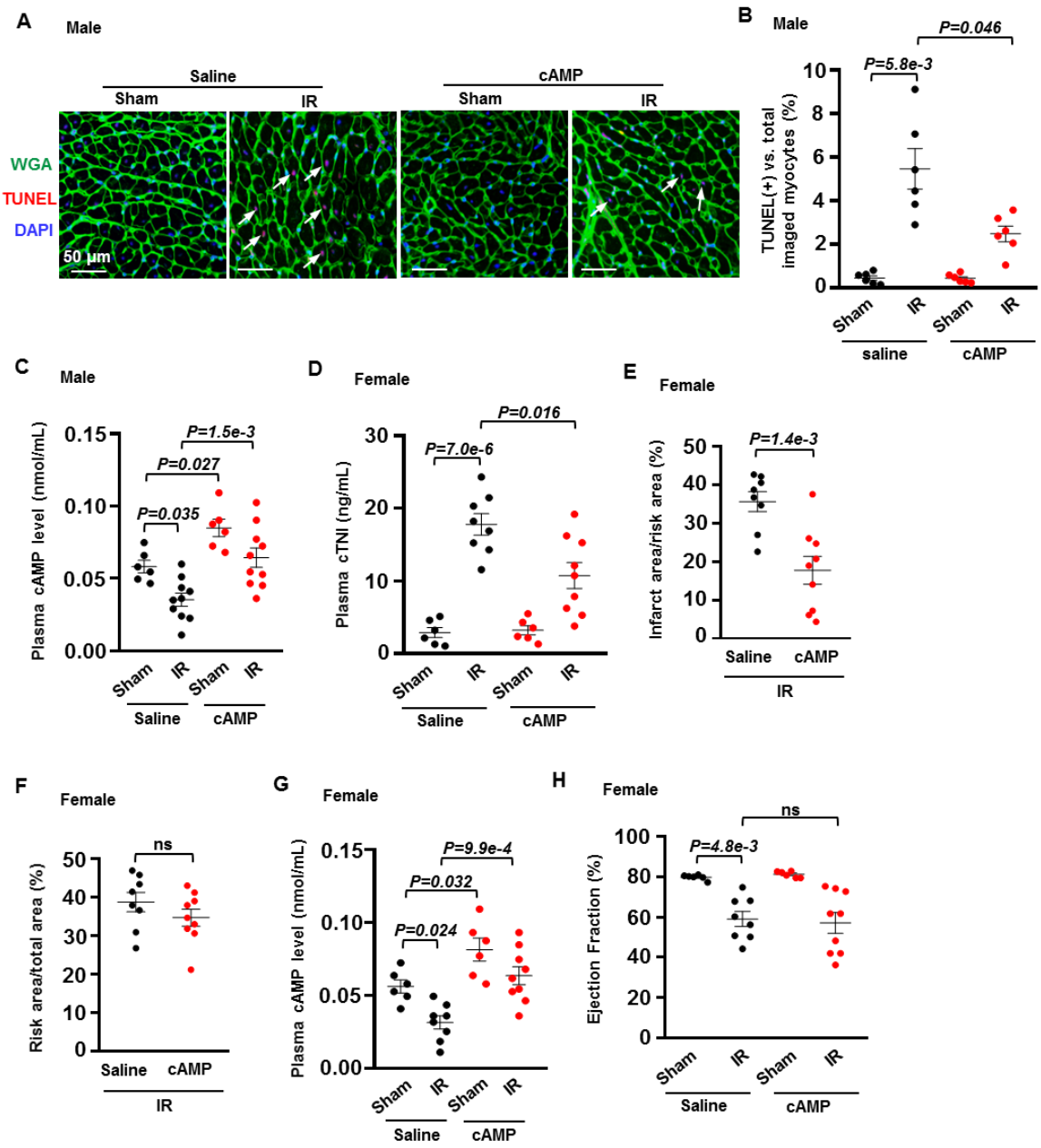
A
Male
Saline
cAMP
Sham
IR
WGA
TUNEL
DAPI
50 μm
B
Male
P=0.046
P=5.8e-3
TUNEL(+) vs. total imaged myocytes (%)
saline
cAMP
C
Male
Plasma cAMP level (nmol/mL)
P=1.5e-3
P=0.027
P=0.035
D
Female
Plasma cTNI (ng/mL)
P=0.016
P=7.0e-6
E
Female
Infarct area/risk area (%)
P=1.4e-3
F
Female
Risk area/total area (%)
ns
G
Female
Plasma cAMP level (nmol/mL)
P=9.9e-4
P=0.032
P=0.024
H
Female
Ejection Fraction (%)
ns
P=4.8e-3

Figure S29. The effect of exogenous cAMP on *in vivo* cardiac IR injury and plasma cAMP level in male or female mice

A and **B**, Images and quantified results of TUNEL staining showing that exogenous membrane impermeable cAMP significantly reduced IR-induced CM apoptosis in male mouse hearts. White arrows indicated apoptotic myocardia with TUNEL-positive nuclei. DAPI indicated nuclei, and WGA indicated the myocardium in the corresponding fields of heart sections, n=6. The representative images were chosen based on their quality and to most accurately reflect the group average across all the available data. **C** and **G**, Results of endpoint plasma cAMP levels in male and female mice. IR mice had significantly decreased plasma cAMP levels In control mice without cAMP administration compared to sham mice. Exogenous cAMP administration significantly increased plasma cAMP levels in both sham and IR mice. After the cAMP treatment, plasma cAMP levels of IR mice were almost equivalent to those of normal mice (sham mice without cAMP treatment), n=6 (Sham/Vehicle), 10 (IR/Vehicle), 6 (Sham/cAMP), and 10 (IR/cAMP) for male mice, n=6 (Sham/Vehicle), 8 (IR/Vehicle), 6 (Sham/cAMP), and 9 (IR/cAMP) for female mice. **D**, Results of plasma cTnI levels showing that cAMP significantly inhibited IR-induced plasma cTnI increase in female mice, n=6 (Sham/Vehicle), 8 (IR/Vehicle), 6 (Sham/cAMP), and 9 (IR/cAMP). **E**, Quantitative results of cardiac TTC staining showing that cAMP significantly reduced IR-induced myocardial infarction in female mice, n=8 (IR/Vehicle) and 9 (IR/cAMP). **F**, Results of the area at risk in female mouse hearts with IR surgery showed no significant difference between IR (saline) and IR (cAMP) groups, which reflects the repeatability and stability of cardiac IR surgery, n=8 (IR/Vehicle) and 9 (IR/cAMP). **H**, Results of cardiac ejection fraction assessed by echocardiogram showing that exogenous cAMP did not significantly affect IR-induced cardiac systolic dysfunction in female mice, n=6 (Sham/Vehicle), 8 (IR/Vehicle), 6 (Sham/cAMP), and 9 (IR/cAMP). The representative images were chosen based on their quality and to most accurately reflect the group average across all the available data. Data were mean ± SEM. Data in **Figures S29C** and **S29G** were analyzed by the one-way ANOVA followed by post-hoc comparisons with Bonferroni corrections for 3 comparisons, **Figures S29B**, **S29D,** and **S29H** by the Welch ANOVA with Dunnett T3 post hoc tests for 2 comparisons, **Figures S29E** and **S29F** by the unpaired t-test. All reported P-values have been adjusted for a predetermined number of multiple comparisons, as specified in the corresponding figures, except in **Figures S29E** and **S29F,** where raw P-values are reported. $P < 0.05$ was statistically significant. ns: no significant difference.

Figure S30

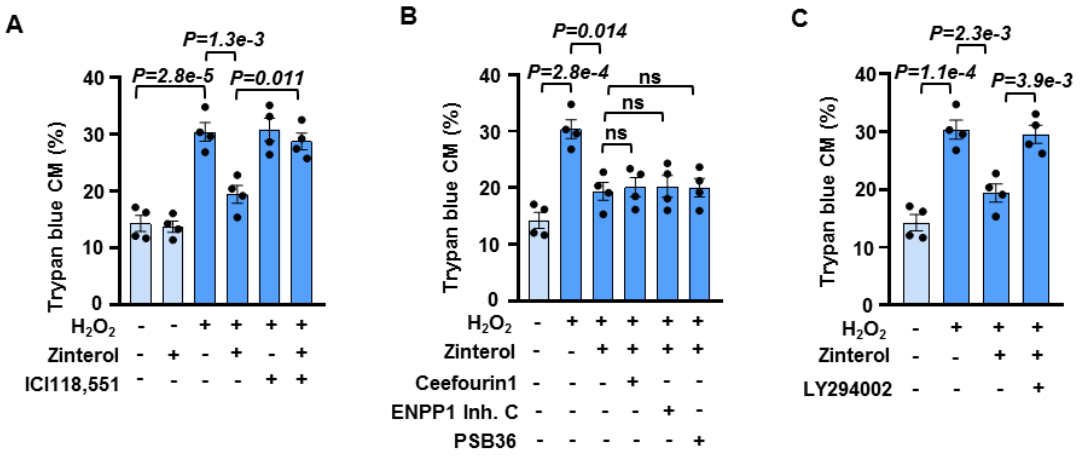

Figure S30. The role of MRP4, ENPP1, A1R, and PI3K in β2AR-mediated CM protection. **A**, Results of trypan blue exclusion assay showing that β2AR agonist zinterol (10 μM) largely attenuated CM death induced by H_2O_2 (5 μM for 24 h), and β2AR antagonist ICI118,551 (0.5 μM) significantly abolished the protective effect of zinterol against H_2O_2-induced CM, n=4. **B**, Results of trypan blue exclusion assay showing that MRP4 inhibitor ceefourin1 (20 μM), ENPP1 inhibitor (ENPP1 inhibitor C, 10 μM), or A1R antagonist PSB36 (10 nM) had no significant effect on the protective effect of zinterol on CM survival, n=4. **C**, Results of trypan blue exclusion assay showing that PI3K inhibitor LY284002 (10 μM) significantly abolished the protective effect of zinterol against H_2O_2-induced CM death, n=4. Data were mean ± SEM. Data in **Figures S30A** and **S30C** were analyzed by the Kruskal-Wallis test followed by Conover-Iman post-hoc test with Bonferroni corrections for 3 comparisons, and **Figure S30B** by the Kruskal-Wallis test followed by Conover-Iman post-hoc test with Bonferroni corrections for 5 comparisons. All reported P-values have been adjusted for a predetermined number of multiple comparisons, as specified in the corresponding figures. P <0.05 was statistically significant. ns: no significant difference.

Figure S31

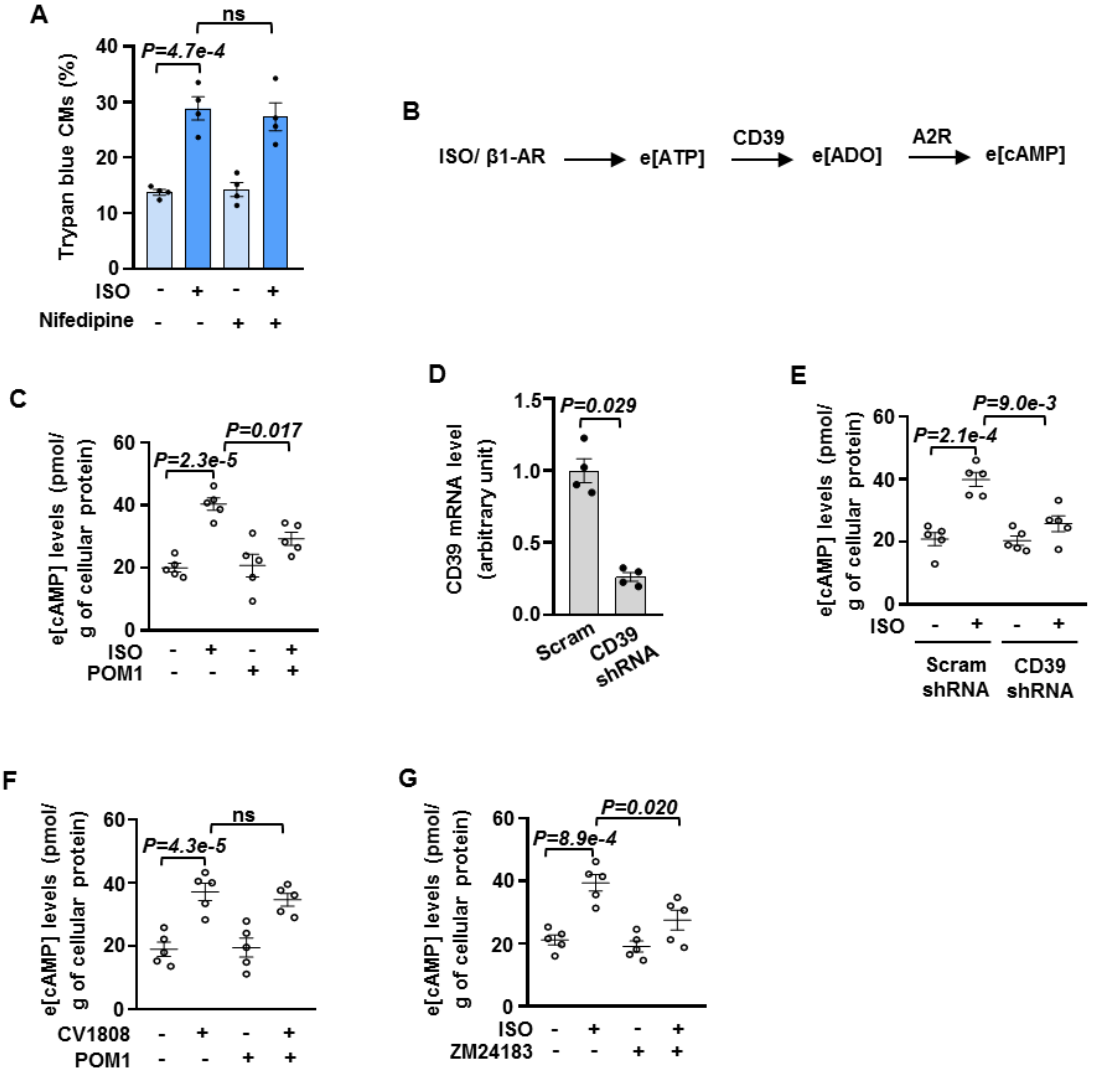
A
ns
P=4.7e-4
Trypan blue CMs (%)
40
30
20
10
0
ISO - + - +
Nifedipine - - + +
B
ISO/ β1-AR
e[ATP]
CD39
e[ADO]
A2R
e[cAMP]
C
P=0.017
P=2.3e-5
e[cAMP] levels (pmol/ g of cellular protein)
60
40
20
0
ISO - + - +
POM1 - - + +
D
P=0.029
CD39 mRNA level (arbitrary unit)
1.5
1.0
0.5
0.0
Scram
CD39 shRNA
E
P=9.0e-3
P=2.1e-4
e[cAMP] levels (pmol/ g of cellular protein)
60
40
20
0
ISO - + - +
Scram shRNA
CD39 shRNA
F
ns
P=4.3e-5
e[cAMP] levels (pmol/ g of cellular protein)
60
40
20
0
CV1808 - + - +
POM1 - - + +
G
P=0.020
P=8.9e-4
e[cAMP] levels (pmol/ g of cellular protein)
60
40
20
0
ISO - + - +
ZM24183 - - + +

Figure S31. The role of L-type Ca^{2+} Channel in ISO-induced CM death; the role of CD39 and A2AR in β1AR- or A2R-induced e[cAMP].

A, Quantitative results of trypan blue exclusion assay showing that L-type Ca^{2+} Channel inhibitor nifedipine (10 μM) did not have a significant effect on CM death induced by ISO (10 μM for 24 h), n=4. **B**, Hypothetical model depicting the mechanism responsible for ISO-induced cAMP efflux from CMs. **C**, Results of e[cAMP] levels in supernatants of CMs showing that CD39 inhibitor POM1 (20 μM) significantly inhibited e[cAMP] elevation induced by ISO (10 μM for 30 min), n=5. **D**, RT-qPCR results showing mRNA levels of CD39 in CMs treated with CD39 shRNA via lentivirus. CD39 shRNA largely reduced CD39 expression, n=4. **E**, Results of e[cAMP] levels in supernatants of CMs showing that CD39 shRNA significantly inhibited ISO-induced cAMP efflux from CMs, n=5. **F**, Results of e[cAMP] levels showing that POM1 did not affect e[cAMP] elevation induced by A2R agonist CV1808 (1 μM for 30 min), n=5. **G**, Results of e[cAMP] levels showing that A2R antagonist ZM24183 (200 nM) significantly inhibited ISO-induced e[cAMP] elevation, n=5. Data were mean ± SEM. Data in **Figures S31A**, **S31C,** and **S31E-S31G** were analyzed by the two-way ART ANOVA with Bonferroni post-hoc test corrections for 2 comparisons, and **Figure S31D** by the Mann-Whitney test. All reported P-values have been adjusted for a predetermined number of multiple comparisons, as specified in the corresponding figures, except in **Figure S31D,** where raw P-value is reported. $P < 0.05$ was statistically significant. ns: no significant difference.